Rapid #: -22138743

TYPE:	Article CC:CCL
JOURNAL TITLE:	Journal of metamorphic geology
USER JOURNAL TITLE:	Journal of Metamorphic Geology
ARTICLE TITLE:	An enlarged and updated internally consistent thermodynamic dataset with uncertainties and correlations: the system K 2 O–Na 2 O–CaO–MgO–MnO–FeO–Fe 2 O 3 –Al 2 O 3 –TiO 2 –SiO 2 –C–H 2 –O 2
ARTICLE AUTHOR:	HOLLAND, T J B
VOLUME:	8
ISSUE:	1
MONTH:	
YEAR:	1990
PAGES:	89 - 124
ISSN:	0263-4929
OCLC #:	

J. metamorphic Geol., 1990, **8**, 89–124

An enlarged and updated internally consistent thermodynamic dataset with uncertainties and correlations: the system K_2O–Na_2O–CaO–MgO–MnO–FeO–Fe_2O_3–Al_2O_3–TiO_2–SiO_2–C–H_2–O_2

T. J. B. HOLLAND
Department of Earth Sciences, University of Cambridge, Downing Street, Cambridge CB2 3EQ, UK

R. POWELL
Department of Geology, University of Melbourne, Parkville, Victoria 3052, Australia

ABSTRACT We present, as a progress report, a revised and much enlarged version of the thermodynamic dataset given earlier (Holland & Powell, 1985). This new set includes data for 123 mineral and fluid end-members made consistent with over 200 P–T–X_{CO_2}–f_{O_2} phase equilibrium experiments. Several improvements and advances have been made, in addition to the increased coverage of mineral phases: the data are now presented in three groups ranked according to reliability; a large number of iron-bearing phases has been included through experimental and, in some cases, natural Fe:Mg partitioning data; H_2O and CO_2 contents of cordierites are accounted for with the solution model of Kurepin (1985); simple Landau theory is used to model lambda anomalies in heat capacity and the Al/Si order–disorder behaviour in some silicates, and Tschermak-substituted end-members have been derived for iron and magnesium end-members of chlorite, talc, muscovite, biotite, pyroxene and amphibole.

For the subset of data which overlap those of Berman (1988), it is encouraging to find both (1) very substantial agreement between the two sets of thermodynamic data and (2) that the two sets reproduce the phase equilibrium experimental brackets to a very similar degree of accuracy. The main differences in the two datasets involve size (123 as compared to 67 end-members), the methods used in data reduction (least squares as compared to linear programming), and the provision for estimation of uncertainties with this dataset. For calculations on mineral assemblages in rocks, we aim to maximize the information available from the dataset, by combining the equilibria from all the reactions which can be written between the end-members in the minerals. For phase diagram calculations, we calculate the compositions of complex solid solutions (together with P and T) involved in invariant, univariant and divariant assemblages. Moreover we strongly believe in attempting to assess the probable uncertainties in calculated equilibria and hence provide a framework for performing simple error propagation in all calculations in THERMOCALC, the computer program we offer for an effective use of the dataset and the calculation methods we advocate.

Key words: internally consistent thermodynamic data set; phase equilibrium calculations; thermodynamic data

List of symbols

$\Delta_f H_{1,298}$ = enthalpy of formation from the elements at 1 bar and 298 K. Units: kJ mol^{-1}
$S_{1,298}$ = entropy at 1 bar and 298 K. Units: kJ K^{-1} mol^{-1}.
$V_{1,298}$ = volume at 1 bar and 298 K. Units: kJ kbar^{-1} mol^{-1}.
C_p = heat capacity; $C_p = a + bT + cT^{-2} + dT^{-1/2}$. Units: kJ K^{-1} mol^{-1}.
α = coefficient of thermal expansion (usually grouped with V as αV). Units: K^{-1}.
β = coefficient of isothermal compressibility (usually grouped with V as βV). Units kbar^{-1}.
$\Delta G°$ = Gibbs free energy change for a reaction among pure end-member phases at the pressure and temperature of interest. Units: kJ mol^{-1}.
R = the gas constant (0.0083143 kJ K^{-1} mol^{-1}).
T = absolute temperature. Units: K.
P = pressure. Units: kbar.
K = equilibrium constant for a balanced reaction. Units: dimensionless

INTRODUCTION

In previous publications (Powell & Holland, 1985; Holland & Powell, 1985; Powell & Holland, 1988: henceforth DS1, DS2 and DS3, respectively) we have presented an internally consistent thermodynamic dataset for end-members of rock-forming minerals, methods of application

Table 1. Formulae of end-members in the dataset, in alphabetical order. In the list, V denotes a site vacancy. The different sites in the mineral formulae are separated and, in some cases, parentheses are used to clarify the grouping of elements which share sites, with tetrahedral sites denoted usually by square brackets. For certain end-members (denoted by *) mixing-on-sites activities according to the above formulae were used in the data extraction process.

ab	equilibrium albite	$Na[AlSi_3]O_8$
abh	high albite	$Na[AlSi_3]O_8$
acm	acmite	$NaFe[Si_2]O_6$
ak	akermanite	$Ca_2[Si_2Mg]O_7$
alm	almandine	$Fe_3Al_2Si_3O_8$
ames	amesite	$Mg_4(Al_2)Si_2[Al_2]O_{10}(OH)_8$*
an	anorthite	$Ca[Al_2Si_2]O_8$
and	andalusite	Al_2SiO_5
andr	andradite	$Ca_3Fe_2Si_3O_8$
ann	annite	$KFe(Fe_2)Si_2[SiAl]O_{10}(OH)_2$*
anth	anthophyllite	$VMg_2Mg_3(Mg_2)Si_4[Si_4]O_{22}(OH)_2$
arag	aragonite	$CaCO_3$
bq	β-quartz	SiO_2
br	brucite	$Mg(OH)_2$
cats	Ca-Tschermak's pyroxene	$CaAl[SiAl]O_6$
cc	calcite	$CaCO_3$
cel	celadonite	$KV(MgAl)Si_2[Si_2]O_{10}(OH)_2$*
chr	chrysotile	$Mg_3Si_2O_5(OH)_4$
clin	clinochlore	$Mg_4(MgAl)Si_2[AlSi]O_{10}(OH)_8$*
coe	coesite	SiO_2
cor	corundum	Al_2O_3
crd	cordierite	$Mg_2[Al_4Si_5]O_{18}$
cumm	cummingtonite	$VMg_2Mg_3(Mg_2)Si_4[Si_4]O_{22}(OH)_2$
cz	clinozoisite	$Ca_2AlAl_2Si_3O_{12}(OH)$*
daph	daphnite	$Fe_4(FeAl)Si_2[AlSi]O_{10}(OH)_8$*
deer	deerite	$Fe_{12}Fe_6Si_{12}O_{40}(OH)_{10}$
di	diopside	$CaMg[Si_2]O_6$
di.o	Pbca-diopside	$CaMg[Si_2]O_6$
dia	diaspore	$AlOOH$
diam	diamond	C
dol	dolomite	$CaMg(CO_3)_2$
east	eastonite	$KMg(MgAl)Si_2[Al_2]O_{10}(OH)_2$*
ed	edenite	$NaCa_2Mg_3(Mg_2)Si_4[Si_3Al]O_{22}(OH)_2$*
en	enstatite	$MgMg[Si_2]O_6$
en.c	C2/c-enstatite	$MgMg[Si_2]O_6$
ep	epidote	$Ca_2FeAl_2Si_3O_{12}(OH)$*
fa	fayalite	Fe_2SiO_4
fame	Fe-amesite	$Fe_4(Al_2)Si_2[Al_2]O_{10}(OH)_8$*
fath	Fe-anthophyllite	$VFe_2Fe_3(Fe_2)Si_4[Si_4]O_{22}(OH)_2$
fcar	Fe-carpholite	$FeAl_2Si_2O_6(OH)_4$
fcel	Fe-celadonite	$KV(FeAl)Si_2[Si_2]O_{10}(OH)_2$*
fcrd	Fe-cordierite	$Fe_2[Al_4Si_5]O_{18}$
fctd	Fe-chloritoid	$FeAl_2SiO_5(OH)_2$
fdol	Fe-dolomite	$CaFe(CO_3)_2$
fgl	Fe-glaucophane	$VNa_2Fe_3(Al_2)Si_4[Si_4]O_{22}(OH)_2$
fhb	Fe-hornblende	$VCa_2Fe_3(FeAl)Si_4[Si_3Al]O_{22}(OH)_2$*
fo	forsterite	Mg_2SiO_4
fs	ferrosilite	$FeFe[Si_2]O_6]$
fst	Fe-staurolite	$Fe_4Al_{18}Si_{7.5}O_{48}H_4$
fta	Fe-talc	$Fe_2FeSi_2[Si_2]O_{10}(OH)_2$*
ftat	Fe-Tschermak's talc	$Fe_2AlSi_2[SiAl]O_{10}(OH)_2$*
ftr	Fe-tremolite	$VCa_2Fe_3(Fe_2)Si_4[Si_4]O_{22}(OH)_2$
geh	gehlenite	$Ca_2[Al_2Si]O_7$

Table 1. (*Continued.*)

gl	glaucophane	$VNa_2Mg_3(Al_2)Si_4[Si_4]O_{22}(OH)_2$
gph	graphite	C
gr	grossular	$Ca_3Al_2Si_3O_8$
grun	grunerite	$VFe_2Fe_3(Fe_2)Si_4[Si_4]O_{22}(OH)_2$
hb	hornblende	$VCa_2Mg_3(MgAl)Si_4[Si_3Al]O_{22}(OH)_2$*
hed	hedenbergite	$CaFe[Si_2]O_6$
hem	hematite	Fe_2O_3
herc	hercynite	$FeAl_2O_4$
ilm	ilmenite	$FeTiO_3$
iron	iron	Fe
jd	jadeite	$NaAl[Si_2]O_6$
kals	kalsilite	$K[AlSi]O_4$
ksp	equilibrium K-feldspar	$K[AlSi_3]O_8$
ky	kyanite	Al_2SiO_5
law	lawsonite	$CaAl_2Si_2O_7(OH)_2{\cdot}H_2O$
lc	leucite	$K[AlSi_2]O_6$
lime	lime	CaO
ma	margarite	$CaV(Al_2)Si_2[Al_2]O_{10}(OH)_2$
mag	magnesite	$MgCO_3$
mang	manganosite	MnO
mcar	Mg-carpholite	$MgAl_2Si_2O_6(OH)_4$
mctd	Mg-chloritoid	$MgAl_2SiO_5(OH)_2$
me	meionite	$Ca_4CO_3[Si_6Al_6]O_{24}$
merw	merwinite	$Ca_3MgSi_2O_8$
mgts	Mg-Tschermak's pyroxene	$MgAl[SiAl]O_6$
mont	monticellite	$CaMgSiO_4$
mrb	magnesioriebeckite	$VNa_2Mg_3(Al_2)Si_4[Si_4]O_{22}(OH)_2$
mst	Mg-staurolite	$Mg_4Al_{18}Si_{7.5}O_{48}H_4$
mt	magnetite	$FeFe_2O_4$
mu	muscovite	$KV(Al_2)Si_2[SiAl]O_{10}(OH)_2$*
naph	Na-phlogopite	$NaMg(Mg_2)Si_2[SiAl]O_{10}(OH)_2$
ne	nepheline	$Na[AlSi]O_4$
pa	paragonite	$NaV(Al_2)Si_2[SiAl]O_{10}(OH)_2$
parg	pargasite	$NaCa_2Mg_3(MgAl)Si_4[Si_2Al_2]O_{22}(OH)_2$*
per	periclase	MgO
phl	phlogopite	$KMg(Mg_2)Si_2[SiAl]O_{10}(OH)_2$*
pre	prehnite	$Ca_2AlSi_2[SiAl]O_{10}(OH)_2$
pswo	pseudo-wollastonite	$CaSiO_3$
pump	pumpellyite	$Ca_4Al_4(MgAl)Si_6O_{21}(OH)_7$
pxmn	pyroxmangite	$MnSiO_3$
py	pyrope	$Mg_3Al_2Si_3O_8$
pyhl	pyrophyllite	$Al_2Si_4O_{10}(OH)_2$
q	α-quartz	SiO_2
rhc	rhodochrosite	$MnCO_3$
rhod	rhodonite	$MnSiO_3$
rnk	rankinite	$Ca_3Si_2O_7$
nu	rutile	TiO_2
san	sanidine	$K[AlSi_3]O_8$
sdph	siderophyllite	$KFe(FeAl)Si_2[Al_2]O_{10}(OH)_2$*
sid	siderite	$FeCO_3$
sill	sillimanite	Al_2SiO_5
sp	spinel	$MgAl_2O_4$
sph	sphene	$CaTiSiO_5$
spu	spurrite	$Ca_4Si_2O_8{\cdot}CaCO_3$
ta	talc	$Mg_2MgSi_2[Si_2]O_{10}(OH)_2$*
tats	Tschermak's talc	$Mg_2AlSi_2[SiAl]O_{10}(OH)_2$*
teph	tephroite	Mn_2SiO_4
tr	tremolite	$VCa_2Mg_3(Mg_2)Si_4[Si_4]O_{22}(OH)_2$
ty	tilleyite	$Ca_3Si_2O_7{\cdot}(CaCO_3)_2$
usp	ulvospinel	$Fe(FeTi)O_4$
vsv	vesuvianite	$Ca_{19}Mg(MgAl_7)Al_4Si_{18}O_{69}(OH)_9$
wo	wollastonite	$CaSiO_3$
zo	zoisite	$Ca_2AlAl_2Si_3O_{12}(OH)$
CH4		CH_4
CO		CO
CO2		CO_2
H2		H_2
H2O		H_2O
O2		O_2

of the dataset, and a computer program (THERMOCALC), which performs calculations on the conditions of equilibration of mineral assemblages in rocks and allows the construction of phase diagrams. As well as being internally consistent, having been generated from high temperature–pressure mineral equilibria experiments, that dataset was in agreement with virtually all the high-temperature calorimetric data available. Thus, with confidence, we could predict mineral equilibria for reactions which have not been determined experimentally; moreover, we were able to estimate the likely uncertainties associated with such predictions, an absolute prerequisite in any (thermodynamic) calculations.

The previously published dataset was presented as a core (DS2, p. 350) of more reliable thermodynamic data, and was intended as a preliminary summary at an early stage in the longer term project. Natural rock assemblages are capable of yielding more information on their conditions of formation if reliable thermodynamic data exist for a larger set of mineral end-members, because it is then possible to define more independent conditions of chemical equilibrium in the mineral assemblage; thus the statistical advantage of the increased information available may be used in assessing *both* the conditions of formation *and* the degree of equilibrium attained in rocks (DS3, p. 190). Moreover, with a larger set of mineral end-members, for phase diagram calculations, we can now calculate the compositions of complex solid solutions (and P,T) involved in-, uni- and divariant equilibria, rather than being restricted to 'end-member' phase diagrams.

In our earlier dataset we presented data for 43 end-members (DS2 appendix A). In this work, which is essentially a progress report, we present new thermodynamic data for a further 80 end-members of common rock-forming minerals, bringing the total number to 123, a near-threefold increase over the original size. The mineral formulae and abbreviations used for the new set are given in Table 1.

THE ENLARGED AND UPDATED DATASET

We have built upon the principles and methods outlined in DS1 and 2; the details will be discussed only where they differ from those presented there, and only a brief resumé of the assumptions made will be given here. For a balanced chemical reaction the equilibrium relation is

$$0 = \Delta G^\circ + RT \ln K.$$

For each end-member mineral phase the free energy contribution to ΔG° is

$$\Delta_f H_{1,298} - TS_{1,298} + \int_{298}^{T} C_p\, dT - T \int_{298}^{T} \frac{C_p}{T}\, dT + [V_{1,298} + \alpha V(T - 298)]P - \frac{\beta V}{2} P^2.$$

For fluid species end-members the volume–pressure integrals are replaced by the term $RT \ln f$, which may be evaluated from the equations given in Table 2.

Table 2. H_2O and CO_2 fugacity polynomials expressed as $RT \ln f$, in units of kJ mol^{-1}; T in Kelvin and P in kilobars.

$RT \ln f = a + bT + cT^2$

$a = a_1 + a_2P + a_3P^2 + a_4P^{-1} + a_5P^{-2}$
$b = b_1 + b_2P + b_3P^{-1} + b_4P^{-2} + b_5P^{-1/2} + b_6P^{-3}$
$c = c_1 + c_2P + c_3P^{-2} + c_4P^{-1/2} + c_5P^{-1} + c_6P^{-3}$

	CO_2		H_2O
a_1	−10.094	a_1	−40.338
a_2	2.6993	a_2	1.6474
a_3	−0.016983	a_3	−0.0062115
a_4	3.2804	a_4	2.0068
a_5	−0.24010	a_5	0.0562929
b_1	0.098597	b_1	0.117372
b_2	0.000865307	b_2	0
b_3	0.0161904	b_3	0
b_4	−0.0021663	b_4	−0.00046710
b_5	−0.046448	b_5	0
b_6	0.000143064	b_6	0
c_1	-3.6780×10^{-6}	c_1	-7.3681×10^{-6}
c_2	-1.189×10^{-7}	c_2	1.10295×10^{-7}
c_3	4.2467×10^{-7}	c_3	-9.8774×10^{-7}
c_4	0	c_4	-2.4819×10^{-5}
c_5	0	c_5	8.2948×10^{-6}
c_6	-3.9520×10^{-8}	c_6	8.33667×10^{-8}

Where mixed volatiles are involved (mixtures of H_2O and CO_2) we assume a non-ideal mixing relation expressed as a subregular model (DS1, p. 332) in order to calculate the activities of the fluid species at high pressure and temperature. As explained in DS1, we make the assumption that all the quantities in the above expressions are either well-known or can be estimated with relatively high precision, and that the term which we need to determine from phase equilibrium experiments is the enthalpy of formation of each mineral end-member.

For each reaction we have determined enthalpy of reaction brackets corresponding to the experimental P–T ($X_{CO_2} f_{O_2}$) brackets. These individual enthalpy of reaction brackets are then processed to give an overall enthalpy of reaction bracket for each reaction (DS1, p. 333–334). The central value and with the width of these overall enthalpy of reaction brackets are used to set up a least squares problem. The goal is to determine a unique set of mineral enthalpies which reproduce, within error, the set of enthalpy brackets discussed above, and hence satisfy the original P–T (X_{CO_2}, f_{O_2}) brackets.

Changes to data extraction methods

As outlined above and in DS1, experimental brackets, such as temperature brackets at a series of pressures, are converted to enthalpy of reaction brackets, assuming that the remaining necessary thermodynamic data are relatively well-known. These enthalpy brackets are converted to one enthalpy bracket, representing this reaction, for inclusion in the least squares analysis. The less robust method of conversion advocated in DS1 has been replaced by taking the median of both the low-enthalpy ends of the brackets and of the high-enthalpy ends of the brackets, the average of these medians giving the preferred value of the enthalpy. The estimated standard deviation on the

preferred enthalpy of reaction is taken as a quarter of the difference between the high and low bracket ends.

Following the appearance of criticisms in the literature of the least squares (LS) approach (Berman, 1988; Berman & Brown, 1987), it is worth reiterating and defending the advantages and validity of the LS method in processing these cumulative enthalpy of reaction brackets (see also DS1, p. 388). One of the main differences between the linear programming (LP) method and our use of LS is that in the LP method, *each* experimental bracket is treated separately, with the fit of the bracket being unconstrained within the bracket; in our method a *cumulative* bracket is represented by its centre, being weighted in the least squares sense according to the bracket width. Thus, the criticism of the least squares method is that it might tend to force the fit towards the centre of the bracket. We feel that this criticism is not justified partly because we use a cumulative bracket and also because the probabilities associated with the experimental bracket are unlikely to be as simple as assumed by the linear programmers. Whereas they assume an equal probability of a result lying anywhere within an experimental bracket, there is a finite probability that the result lies outside the bracket, or indeed, that the bracket is too wide; this is because the limits of experimental brackets are subject to experimental error. Moreover, from kinetic considerations, the value is less likely to be very close to the limits of the experimental bracket.

The probability curve is thus more likely to be bell-shaped, with a flat top whose width relates to the width of the bracket in relation to the experimental uncertainties (Demarest & Haselton, 1981). Indeed, ignoring the fuzziness associated with the limits of experimental brackets is one reason why the linear programmers have had to widen more or less arbitrarily the experimental brackets in order to create a feasible region in their analyses. In our approach of combining the enthalpy of reaction brackets into a cumulative bracket, the probability curve for this overall enthalpy of reacton bracket is given by multiplying together the probability curves of the component enthalpy of reaction brackets. The resulting probability distribution, even where the individual component brackets may have flat-topped distributions, will tend to be bell-shaped with only a narrow flat top or, more probably, without a flat top. Moreover, thinking about the cumulative enthalpy bracket in another way, the boundaries of the bracket are uncertain, not only because of the spread of values used for the medians (see earlier), but also because each of these values is uncertain from the experimental uncertainties. Again, the probability curve tends to be bell-shaped. As long as this probability curve does not have a flat top which is wide compared with the bracket width, the use of least squares will be valid. If the width of the bracket is not much wider than the experimental uncertainty on its ends (i.e. $d/s < 2$ in the nomenclature of Demarest & Haselton, 1981; DS1, p. 334) use of the least squares method is certainly justified because the probability distribution is close to Gaussian. In the diagnostic d/s referred to above, d is the half-width of the overall enthalpy of reaction bracket and s is the uncertainty in the location of the bracket ends. Moreover the use of the bracket with width as a weighting in the least squares will tend to minimize the damage caused by a flat top on the probability curve when $d/s \approx 2$ or even $d/s > 2$: the larger the bracket width, the more down-weighted is the reaction, and the less the reaction can contribute to the least squares analysis anyway.

The use of regression diagnostics (Belsley, Kuh & Welsch, 1980) together with new diagnostics discussed below can signal the forcing of a fitted enthalpy to be central to a bracket; in fact, no reaction with large d/s is indicated in Table 8. The majority of the reactions in Table 5 have d/s values less than 2, so the least squares method does appear to work with few problems. We feel that the criticisms of LS are largely illusory because in our experience the method has been demonstrably successful in fitting almost all the available experimental data within their uncertainty limits; additionally, the calculated error bounds at the 2σ level for individual reactions are very similar to the experimental bracket widths. Both LS and LP are capable of providing reliable and similar analyses of the experimental data, each with its advantages and disadvantages. However, we believe that the ability of the least squares method to provide the uncertainties, and their mutual correlations, of the calculated thermodynamic data makes this the preferable method of analysis.

Several levels of reliability are now involved in the data used in the least squares analysis, in particular, for reactions involving phases whose entropies cannot be estimated reliably because of, for instance, Al–Si disorder. For these reactions the overall enthalpy of reaction bracket has been arbitrarily widened, by a factor of up to 3, thus down-weighting every such experimental constraint.

As an aid in the data extraction process, some regression diagnostics (for a general discussion of this topic see Belsey *et al.*, 1980), specifically designed for this analysis, have been used. The sensitivity of the estimated enthalpy of formation of an end-member, $\Delta_f H$, to the enthalpy of the reaction, ΔH_R, is examined in three ways:

(a) via the change in $\Delta_f H$ which is a consequence of doubling the width of a ΔH_R bracket, scaled to an 'expected' $\sigma(\Delta_f H)$ using 0.15 kJ/atom. Rather than give all the values, only the values above a cut-off are presented; a cut-off of 0.25 is used;

(b) via the change in the uncertainty on $\Delta_f H$, $\sigma(\Delta_f H)$, which is a consequence of doubling the width of a ΔH_R bracket, scaled to $\sigma(\Delta_f H)$ for the undoubled ΔH_R bracket. A cut-off of 0.05 is used for the absolute value of this diagnostic;

(c) via the change in Δ_fH on moving a ΔH_R bracket by one quarter of its width, scaled to an 'expected' $\sigma(\Delta_f H)$, using 0.15 kJ/atom, and using a cut-off of 0.25.

All of these diagnostics can be calculated from intermediate results and the least squares solution itself, and are presented in Table 8. The algebraic derivation of these diagnostics is available from RP on request. These diagnostics have been valuable in signalling potential (and real) problems in individual experimental studies. For

example, large values for diagnostics (a) and (c) indicate that the enthalpies of these end-members are strongly influenced by the reaction, while a large positive value for diagnostic (b) indicates that the (small) size of the uncertainty on the enthalpies of these end-members is strongly influenced by this reaction. Large values for diagnostic (a) may indicate aberrance of this reaction *or* competing influences (for instance calorimetric constraints in the case of diam = gph; or the influence of other experimental data on the calculated position of en + 2mag = 2fo + $2CO_2$). Large values for diagnostics (b) and (c) indicate different aspects of the importance of these reactions for the enthalpies of the corresponding end-members, and do not indicate aberrance.

Changes to the existing data

A few changes have been made which slightly alter the results presented in DS2. The fugacity polynomials for CO_2 and H_2O have been improved so that they both cover an extended range (0.1–40 kbar, 300–1200 °C for H_2O and 0.1–k40 kbar, 300–1400 °C for CO_2). The new equation and polynomial terms are given in Table 2. Apart from the extended range of validity, the equations yield essentially identical results to those discussed in detail and displayed graphically in DS1.

The entropy of clinochlore has been measured calorimetrically (Henderson, Essene, Anovitz, Westrum, Hemingway & Bowman, 1983) and is much lower than the value used in DS2. Although the value used there was consistent with the mineral equilibrium studies used in that least squares analysis, that value is inconsistent with the slopes of a large number of reactions involving cordierite, as pointed out by Berman (1988) in his recent review. In contrast, the new value is consistent with these reactions. The entropy and heat capacity of grossular have also been changed; we now use, following the arguments of Berman (1988), the data measured for natural garnet in preference to those for synthetic garnet, although the differences are minor. The entropy of meionite has been reduced to 720 J K^{-1} to make it consistent with the Na/Ca exchange equilibria determined experimentally by Goldsmith & Newton (1977).

Other subtle differences between the dataset in DS2 and that presented here are induced by the change in the method of calculation of the enthalpy of reaction brackets, outlined above, and by the least squares analysis of the new experimental and calorimetric constraints.

Anchors and calorimetric data

In DS2, it was regarded as crucial to incorporate the minimum of calorimetric data in the least squares analysis, so that as much as possible of these data, particularly from high-*T* oxide-melt calorimetry, might provide an independent test of the dataset. This minumum of calorimetric data involved just one end-member for each chemical component of the dataset system; these were the so-called *anchors* of the dataset. With the demonstration of the consistency of the phase equilibrium data with most of the calorimetric measurements (Holland & Powell, 1985; Berman, 1988), the anchor approach is no longer needed and most of the data from acid calorimetry and high-*T* oxide-melt calorimetry are now included as separate calorimetric constraints (Tables 3 and 4).

Table 3. Direct calorimetry constraints used in the fitting process. The data were taken from the compilation of Robie, Hemingway & Fisher 1979, with the exception of anorthite from Carpenter, McConnell & Navrotsky 1985. Units: kJ mol^{-1}.

	$\Delta H_f(1,298)$	σ
ksp	−3967.70	3.30
san	−3959.56	1.68
an	−4231.90	2.50
jd	−3029.94	2.10
fa	−1479.40	2.40
br	−924.50	1.00
dia	−1000.60	3.00
pyhl	−5643.76	4.40
cc	−1207.40	1.70
arag	−1207.40	1.40
mag	−1113.30	1.30
dol	−2324.50	1.70
mt	−1115.73	2.10
lime	−635.09	0.88
ru	−944.75	0.63
per	−601.49	0.30
mang	−385.22	0.46
cor	−1675.70	0.65
hem	−824.60	1.30
q	−910.70	0.50
iron	0.00	0.00
gph	0.00	0.00
diam	1.90	0.20
O_2	0.00	0.00
H_2	0.00	0.00

New data added to the dataset

We have added a further 80 end-members to the earlier core dataset, bringing the total to 123. Most of these could have been added using the methods of DS1 and 2; however, a few have required additions or modifications to the processing. Where entropies have not been measured, the new algorithm of Holland (1989) has been used to estimate third-law values. As in DS1, we have added the required minimum configurational increment to the third-law entropy in order to achieve agreement with experimental phase equilibria.

The dataset extraction now involves experimentally determined solid solution equilibria between minerals, particularly Tschermak ($MgSiAl_{-1}Al_{-1}$) and ferromagnesian ($MgFe_{-1}$) substitutions. In fact, we have found it necessary to include the Tschermak substitutions in talc, chlorite, muscovite, biotite, pyroxenes and calcic amphiboles in order to satisfy the experimental phase relations. In all such calculations ideal mixing on sites was assumed for mineral solid solutions according to the formulae in Table 1, with the exception of aluminous pyroxenes for which ideal charge balance was assumed. These aspects of the dataset are discussed at greater length in the next section.

Some iron-bearing minerals (iron, hem, mt) have lambda heat capacity anomalies at temperatures above 298 K due to magnetic disordering. In order to model the high-temperature thermodynamics, we have taken simple Landau theory for tricritical behaviour to describe the heat

Table 4. Oxide and reaction calorimetry. Units: kJ mol^{-1}. (a) Relative to oxides in borate melt solution calorimetry. Refs: Holm & Kleppa, 1966 (sill, and, ky); Charlu *et al.*, 1975 (py, fo, crd); Brousse *et al.*, 1984 (en, fo, ak, merw, mont); Charlu *et al.*, 1978 (wo, pswo, di, gr); Charlu *et al.*, 1981 (geh). (b) Relative to elements. Heats of formation from the elements from Robie *et al.*, 1979. (c) Reaction 'calorimetry': the enthalpies of the first four reactions were taken to be zero with uncertainties of $\sigma = \pm 1$ kJ per mol $FeMg_{-1}$ exchange, thus assuming near linear dependence of end-members ftr, sdph, fame, ftat on the other end-members in the relevant reactions. Enthalpies for en.c = en and di.o = di are from Holland *et al.*, 1979 and Lindsley, 1981.

(a) Relative to oxides.

Mineral	T(°C)	ΔH_{cal}	σ	ΔH_{298}
sill	697	−2.4	0.6	−0.8
py	697	−79.9	4.6	−79.4
fo	800	−59.5	1.9	−59.7
en	800	−67.8	3.5	−71.5
mont	800	−104.8	1.7	−105.3
ak	800	−178.2	1.6	−176.2
merw	800	−213.8	2.0	−211.4
crd	697	−68.1	3.0	−62.2
di	697	−146.4	1.7	−147.4
wo	697	−89.9	1.5	−89.8
pswo	697	−83.3	1.3	−82.4
geh	697	−128.2	1.3	−124.0
ky	701	−6.2	1.2	−7.9
and	701	−2.8	1.0	−3.9

(b) Relative to elements.

Reaction	T(°C)	ΔH_{cal}	σ
$C + O_2 = CO_2$	25	−393.5	0.1
$H_2 + \frac{1}{2}O_2 = H_2O$	25	−241.8	0.0
$C + 2H_2 = CH_4$	25	−74.8	0.3
$C + \frac{1}{2}O_2 = CO$	25	−110.5	0.2

(c) Reaction 'calorimetry'.

Reaction	T(°C)	ΔH_{298}	σ
4 ftr + 5 hb = 4 tr + 5 fhb	25	0.0	5.0
3 sdph + phl = 3 east + ann	25	0.0	3.0
5 fame + 4 clin = 5 ames + 4 daph	25	0.0	5.0
3 ftat + 2 ta = 3 tats + 2 fta	25	0.0	3.0
en.c = en	25	−6.1	2.0
di.o = di	25	−7.4	2.0

capacity lambda anomalies. While this is only approximate, and an empirical device (it fails to explain the small excess heat capacity just above the critical temperature), the Landau model is both successful and practical in accounting for such heat capacity anomalies. A typical example, for magnetite, is shown in Fig. 1.

Although Landau theory is usually used to describe departure from the high-temperature, disordered state, we will use the petrological convention and describe the excess properties relative to the low-temperature, ordered state:

$$\text{for } T < T_c \quad C_p^{ex} = \frac{TS_{max}}{2\sqrt{T_c}}(T_c - T)^{-1/2}$$

$$S^{ex} = S_{max}(1 - Q^2)$$

$$H^{ex} = 2S_{max}T_c\left(\frac{Q^6}{6} - \frac{Q^2}{2} + \frac{1}{3}\right),$$

$$\text{where} \quad Q = \left(1 - \frac{T}{T_c}\right)^{1/4}$$

$$\text{for } T > T_c, \quad S_{ex} = S_{max}, \quad H_{ex} = \tfrac{2}{3}S_{max}T_c, \quad Q = 0,$$

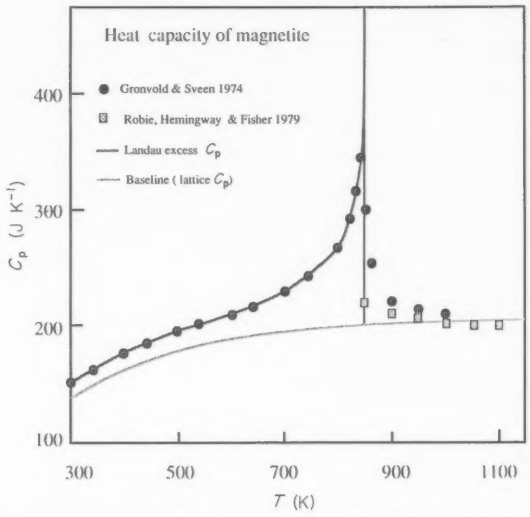

Fig. 1. Heat capacity of magnetite showing the lambda anomaly at 855 K and the Landau model used to represent it.

where T_c is the critical temperature of the phase transition, S_{max} is the maximum entropy due to the phase transition, and S^{ex} and H^{ex} are the entropy and enthalpy of disorder at any temperature T; Q is the macroscopic order parameter which is related to the free energy (of ordering) in conventional Landau terms by the expression

$$\Delta G^{ord} = -\frac{a}{2}(T_c - T)Q^2 + \tfrac{1}{8}cQ^6; \quad T_c = \frac{c}{a}; \quad S_{max} = \frac{a}{2}.$$

The Landau terms, S_{max} and T_c, are given in Table 7. The same Landau formalism can be used to describe Al–Si order–disorder, as discussed by Carpenter (1988); here we use it to describe the equilibrium behaviour of albite (ab), potassium feldspar (ksp), nepheline (ne) and leucite (lc). For ne and lc the Landau parameters were retrieved from measured heat capacities, whereas those for ab and ksp were taken from Carpenter's estimates of T_c, coupled with S_{max}, taken to be about three-quarters of the maximum configurational entropy. For albite, this simplification approximates the behaviour shown by Salje, Kuscholke, Wruck & Kroll (1985), and is quite adequate for most phase equilibrium calculations.

Fe/Mg partitioning experiments among pairs of silicate minerals have been used to extract enthalpies for a number of Fe-silicate and carbonate end-members (see Appendix A for details). For certain important mineral end-members no phase equilibrium experiments are available, and we have resorted to using Fe/Mg or Al/Fe^{3+} partitioning found in nature, together with reasonable estimates for temperature and pressure of formation, to retrieve enthalpies of formation. While this has proved a useful preliminary procedure, the data derived in this way should not be used to estimate rock temperatures through exchange thermometry, because of the obvious circular reasoning. However, these data may be quite robust in

calculations of net transfer reactions and for average pressure calculations on rocks, as described in DS3.

An example of the potential power of this line of reasoning is the extraction of thermodynamic data for siderite and ferrodolomite. The experimental data consist of phase equilibrium experiments on the reactions sid + hem = mt + CO_2 and sid = mt + gph + CO_2; the low-pressure experiments of French (1971) and Weidner (1972) are mutually inconsistent as well as not being in agreement with the measured entropy and volume data (Appendix A), whereas Weidner's high-pressure brackets do agree with the calculated P–T slopes. In an attempt to reconcile these data with the experimental partitioning of Fe and Mg between siderite and ankerite (again two mutually inconsistent studies, Goldsmith, Witters & Northrup, 1962 and Rosenberg 1967; for a useful discussion see Anovitz & Essene 1987), we used natural Fe:Mg partitioning data for pyroxene/ankerite pairs (Klein 1978) and siderite/ankerite pairs (Anovitz & Essene 1987) to help discriminate among the available competing sets of experimental data. The result is that the natural data are in excellent agreement with the experimental data of Rosenberg (1987) and the high-pressure experiments (>4 kbar) of Weidner (1972) but are inconsistent with the experimental results of Goldsmith, Witters & Northrup (1962) and French (1971). Furthermore, the Fe:Mg partitioning data for natural dolomite/diopside pairs (Rice 1977) and dolomite/biotite pairs (Klein 1978) are in very good agreement with these results and the P,T location of our siderite breakdown reactions is almost identical to that deduced by Miyano & Klein (1986). Thus it is possible to use natural mineral compositions together with good estimates of equilibration temperatures to help constrain thermodynamic data and to discriminate among inconsistencies in experimental data.

The new dataset contains data for anhydrous Mg- and Fe-cordierite, derived from experimentally determined phase equilibria and the simple model for hydration and carbonation in cordierite described by Newton & Wood (1979) and extended by Kurepin (1985). Thus the reduction of the activity of anhydrous cordierite end-members in hydrous experimentally produced cordierites could be calculated. In the absence of data, we have assumed that Fe-cordierite behaves identically to Mg-cordierite in its uptake of volatiles, and have taken the equations directly from Kurepin (1985).

In this dataset we provide two sets of clinozoisite data cz and czl. Data for czl is essentially that of Holland & Powell (1985) and is based on the experiments of Jenkins, Newton & Goldsmith (1983). The data for cz is based on the experiments of Holland (1984) where kinetic extrapolation at 15 kbar leads to the conclusion that the cz/zo transformation occurs at around 500 °C (as opposed to <200 °C in Jenkins *et al.*, 1983). At present this problem is unresolved and we suggest that both alternatives be used in calculations on natural rocks, with a view to comparing and evaluating the effects of the two different assumptions. We have found good agreement in barometry with *cz* (as opposed to *czl*) with our limited data, but this may not be everyone's experience.

TSCHERMAK SUBSTITUTIONS

Several phases are characterized by a substitution of Al + Al for [Mg + Fe] + Si over a wide range in compositions as a function of pressure, temperature and mineral assemblage. We feel that it is important to make a start in characterizing and understanding the controls on this substitution, and so we have attempted to derive a thermodynamic data for the following phases:

white micas	(mu, cel, fcel)
biotites	(phl, ann, east, sdph)
chlorites	(clin, daph, ames, fame)
talc	(ta, fta, tats, ftat)
amphiboles	(tr, ftr, hb, fhb)
pyroxenes	(en, mgts, di, cats).

A detailed presentation of the methods used and some applications will be presented elsewhere (T. J. B. Holland and R. Powell, unpublished data). The data used are admittedly scanty, but we feel that a start in this direction is badly needed and that our results are quite encouraging. The equilibria used for these end-members can be found in Tables 4 and 5 together with references for sources of the phases concerned and the compositional data. The small amount of data gained carefully by Jenkins (1983) and Jenkins & Chernosky (1986) have been of enormous value and allow the prediction of the composition of chlorite in all the experiments listed in Table 5.

We have found that chlorites can vary (in common assemblages) from much less aluminous than clinochlore to close to amesite in composition, and we have used iterative refinement in the least squares process to calculate the chlorite composition for each experimental P–T bracket. The compositional changes with pressure, temperature and assemblage make good sense and also agree nicely with natural whiteschist occurences (e.g. Kulke & Schreyer, 1973), for example. We thus avoid the arbitrary, and in several cases somewhat unlikely, assumptions made by Berman (1988) who assumed a constant clinochlore activity of 0.7 in order to reduce the discrepancies between his dataset and certain chlorite experiments. As one might anticipate it is not the assemblages with, for instance, fo + sp + en or sp + py + fo that involve the most aluminous chlorites (typically $clinochlore_{80}$ $amesite_{20}$), but assemblages like crd + cor + chl or chl + and + q (with compositions up to $clinochlore_{40}$ $amesite_{60}$). Figure 2 shows an example of the calculated chlorite compositions and P–T curves for two typical experimentally determined univariant reactions. Berman (1988, p. 496, and fig. 31) noted that he had to increase the entropy of cordierite by nearly 11 J K^{-1} to fit the experimental slopes of such reactions involving aluminosilicates and chlorite. By allowing chlorite composition to vary, and using the calculated compositions in our fitting process, we have found no need to appeal to an excess disordering entropy in cordierite.

The situation for micas, talc and amphiboles is analogous but the primary data are very scarce (see Tables 4 and 5 for details). We would be interested to receive

Table 5. The experimental dataset used in condensed form: rfac is the weighting factor applied (see tex
calculated enthalpy; σ is the calculated uncertainty in enthalpy; uH is the enthalpy uncertainty due to in
parameter as defined in DS2; $h(i)$ is the hat value from the regression indicating the influence of the exp
(e.g. the case of a single reaction being used to determine the enthalpy of an end-member) to h near zer
the degree of misfit with the experiment (see text). ack—activity corrected equilibrium constants: 1 = ca
enstatite; 3 = aluminous chlorite; 4 = aluminous talc; 5 = aluminous hornblende, orthopyroxene and cli
clinopyroxene; 9 = edenite activity in pargasite composition amphibole; 10 = Ca–Fe garnet; 11 = magne
14 = reduced activities (experimental); 15 = reduced activities (natural). Ideal mixing assumed. Refs: B
al., 1984; CM 84 = Chopin & Monié, 1984; EK 81 = Eggert & Kerrick, 1981; G 80 = Goldsmith, 1980;
84 = Gasparik & Newton, 1984; HHL 75 = Huckenholz *et al.*, 1975; HL 77 = Holdaway & Lee, 1977; H
JC86 = Jenkins & Chernosky, 1986; JGN83 = Jenkins *et al.*, 1983; JK 81 = Jacobs & Kerrick, 1981; M 8
RBG 68 = Richardson *et al.*, 1968; RGB 69 = Richardson *et al.*, 1969; S 71 = Skippen, 1971; SKB 82 =

	Reaction	rfac	low	high	calc
1	diam = gph		-2.23	-2.14	-2.18
2	q = bq		1.72	1.75	1.73
3	coe = q		-2.68	-2.59	-2.64
4	pyhl + 6dia = 4and + 4H2O	3.0	302.55	307.65	306.43
5	2dia = cor + H2O	3.0	81.32	82.45	81.73
6	pyhl = and + 3q + H2O	3.0	74.95	75.93	75.47
7	ky = and		3.98	4.21	4.06
8	ky = sill		8.41	8.76	8.66
9	jd + q = abh		10.89	12.08	11.61
10	jd + q = ab		2.35	3.48	2.88
11	pa = jd + ky + H2O		80.53	81.50	81.07
12	pa = abh + cor + H2O		101.66	102.94	101.48
13	pa + q = abh + and + H2O		96.04	97.26	96.75
14	pa + q = abh + ky + H2O		91.57	92.79	92.69
15	2jd = ne + abh		24.14	26.48	25.31
16	mu = san + cor + H2O		104.73	105.94	105.04
17	mu + q = san + and + H2O		99.38	100.52	100.30
18	mu + q = san + sill + H2O		104.52	105.82	104.89
19	mu = ksp + cor + H2O		93.97	95.13	94.48
20	mu + q = ksp + and + H2O		88.84	90.03	89.74
21	mu + q = ksp + sill + H2O		93.95	95.19	94.34
22	wo = pswo		3.05	3.07	3.06
23	cc = lime + CO2		180.89	183.20	180.00
24	cc + bq = wo + CO2		89.54	90.91	90.19
25	cc + bq = wo + CO2		88.54	89.88	90.19
26	cc + bq = wo + CO2	2.0	88.77	90.17	90.19
27	4zo + q = 5an + gr + 2H2O		207.87	212.52	209.88
28	4zo + q = 5an + gr + 2H2O		208.05	213.06	209.88
29	6zo = 6an + 2gr + cor + 3H2O		303.35	309.85	302.85
30	2zo + CO2 = 3an + cc + H2O		37.60	38.97	38.05
31	gr + 2ky + q = 3an		38.65	42.80	41.53
32	gr + 2ky + q = 3an		41.48	48.72	41.53
33	gr + 2ky + bq = 3an		39.78	43.83	39.79
34	2czl + ky + q = 4an + H2O		125.12	129.50	127.31
35	cz = zo		4.77	4.86	4.81
36	gr + q = an + 2wo		49.97	51.17	50.07
37	gr + bq = an + 2wo		47.53	49.22	48.34
38	2zo + ky + q = 4an + H2O		120.88	126.28	125.70
39	2zo + sill + q = 4an + H2O		112.91	117.27	117.05
40	gr + cor = geh + an		104.76	106.58	104.02
41	2gr = 3wo + geh + an		163.00	165.90	167.16
42	gr + 2cor = 3cats	2.0	72.35	73.72	72.84
43	gr + 3cats = 2an + 2geh	2.0	130.97	137.24	135.21

(see text); low, high and calc are the enthalpy brackets used in the least squares and the due to individual pressure and temperature measurement uncertainty; d/s is a bracket width of the experiment on the overall fit, with h ranging from $h = 1.0$ indicating extreme influence near zero for reactions having minimal influence on the least squares results; 'miss' indicates ts: 1 = calcite coexisting with dolomite, data from Gordon & Greenwood 1971; 2 = aluminous e and clinopyroxene; 6 = phengitic muscovite; 7 = aluminous biotite; 8 = aluminous = magnetite in hercynite; 12 = Fe/Mg partition (experimental); 13 = Fe/Mg partition (natural); Refs: BE 63 = Barnes & Ernst, 1963; CDC 85 = Chernosky *et al.*, 1985; CJL 84 = Chatterjee n, 1980; GG 70 = Gordon & Greenwood, 1970; GH 62 = Goldsmith & Heard, 1962; GN 1977; HW 75 = Huang & Wyllie, 1975; IHW 77 = Irving *et al.*, 1977; J84 = Johannes, 1984; 981; M 86 = Miller, 1986; MP 71 = Metz & Puhan, 1971; MS 87 = Massonne & Schreyer, 1987; KB 82 = Schramke *et al.*, 1982; SKW 75 = Slaughter *et al.*, 1975.

calc	σ	uH	d/s	h(i)	ack	miss	Ref
-2.18	0.04	0.03	0.9	0.99			Kennedy & Kennedy 76
1.73	0.02	0.01	0.7	0.98			Mirwald & Massonne 80
-2.64	0.04	0.03	-0.9	1.00			Bohlen & Boettcher 82
06.43	3.80	1.43	1.8	0.33			Haas & Holdaway 73
81.73	1.23	0.38	0.7	0.69			Haas 72
75.47	1.25	0.33	0.9	0.95			Haas & Holdaway 73
4.06	0.10	0.08	0.1	0.91			Newton 66, RGB 69, Holdaway 71
8.66	0.12	0.12	1.1	0.65			Newton 66, RBG 68, Holdaway 71
11.61	0.37	0.40	1.0	0.51			Holland 80
2.88	0.49	0.38	0.7	1.00			Newton & Smith 67, Holland 80
81.07	0.35	0.22	2.3	0.67			Holland 79
01.48	0.33	0.43	-0.8	0.35		-0.54	Chatterjee 70
96.75	0.29	0.41	0.5	0.31			Chatterjee 71
92.69	0.29	0.33	1.8	0.30			Chatterjee 71
25.31	1.02	0.78	1.1	1.00			Robertson et al.57,Gasparik 85
05.04	0.33	0.40	0.0	0.40			Chatterjee & Johannes 74
00.30	0.31	0.38	0.9	0.39			Chatterjee & Johannes 74
04.89	0.31	0.43	0.0	0.31			Chatterjee & Johannes 74
94.48	0.33	0.39	-0.7	0.44			Chatterjee & Johannes 74
89.74	0.32	0.40	0.3	0.38			Chatterjee & Johannes 74
94.34	0.32	0.41	-0.7	0.36			Chatterjee & Johannes 74
3.06	0.01	0.01	2.0	1.00			Osborn & Shairer 41, HW 75
80.00	0.55	0.63	1.8	0.31		-1.61	Smyth & Adams 23
90.19	0.26	0.46	0.7	0.20			Jacobs & Kerrick 81
90.19	0.26	0.45	-0.2	0.20		1.18	Ziegenbein & Johannes 74
90.19	0.26	0.47	-0.5	0.05		0.06	Haselton et al. 78
09.88	0.81	1.55	-1.6	0.16			Boettcher 70,Newton 66, CJL 84
09.88	0.81	1.67	0.2	0.14			Newton 66
02.85	1.34	2.17	0.2	0.23		-0.37	Boettcher 70,Newton 66, CJL 84
38.05	0.42	0.46	0.8	0.50			Allen & Fawcett 82
41.53	0.83	1.38	0.1	0.21			Koziol & Newton 87
41.53	0.83	1.38	2.6	0.07			Goldsmith 80
39.79	0.83	1.35	0.8	0.22			Koziol & Newton 87, G 80
27.31	1.90	1.46	0.8	1.00			Jenkins et al. 83
4.81	0.04	0.03	1.3	1.00			Holland 84
50.07	0.37	0.40	1.1	0.50			Huckenholz et al 75, Newton 66
48.34	0.37	0.56	0.2	0.25			HHL 75, Newton 66, Hays 67
25.70	0.53	1.80	0.3	0.05			Goldsmith 81, JGN 83, J 84
17.05	0.54	1.45	0.2	0.08			Newton 66, Newton & Kennedy 63
04.02	0.59	0.61	0.0	0.56		-1.25	Boettcher 70, HHL 75
67.16	0.78	0.96	0.8	0.39		1.62	Hays 67, Huckenholz et al. 75
72.84	0.98	0.45	0.2	0.69			Gasparik 84
35.21	1.36	1.43	2.2	0.06			Hays 67

Table 5. (*Continued.*)

Reaction	rfac	low	high	calc
44 3cats = an + geh + cor	2.0	30.72	32.70	31.18
45 gr + 3ky = 3an + cor	2.5	51.69	57.15	50.32
46 3cc + an + cor = 2geh + 3CO2	2.0	391.53	397.77	396.74
47 2cc + an = wo + geh + 2CO2	2.0	246.05	249.49	250.87
48 an + cor + 3cc = 2geh + 3CO2	2.0	390.33	397.27	396.74
49 an + 2cc = geh + wo + 2CO2	2.0	241.60	246.52	250.87
50 4ma = 2zo + 2ky + 3cor + 3H2O		227.63	230.72	230.95
51 ma = an + cor + H2O		90.94	92.14	91.36
52 ma = an + cor + H2O	2.0	90.38	91.59	91.36
53 ma + q = an + ky + H2O	2.0	81.83	82.85	82.57
54 4ma + 3q = 2zo + 5ky + 3H2O		204.60	206.78	204.56
55 ma + q = an + and + H2O	2.0	84.98	86.17	86.62
56 ma + q = an + ky + H2O	2.0	81.94	82.95	82.57
57 law = an + 2H2O		148.33	151.90	151.71
58 5law = 2zo + ma + 2q + 8H2O	2.0	547.09	554.74	550.26
59 4law = 2zo + ky + q + 7H2O	2.0	478.18	483.70	481.12
60 5pre = 2zo + 2gr + 3q + 4H2O	2.0	229.86	231.55	230.71
61 3an + cc = me		34.50	34.99	34.74
62 3cc + 2wo = ty + CO2	2.0	122.47	124.07	123.89
63 ty = spu + CO2	2.0	136.95	138.66	138.51
64 spu + 4wo = 3rnk + CO2	2.0	802.67	829.46	816.06
65 2fo + 2ta = 5en + 2H2O		201.90	204.67	203.66
66 2ta = 3en + 2bq + 2H2O		218.02	220.93	220.56
67 2ta = 3en + 2q + 2H2O		214.45	216.43	217.09
68 2anth = 7en + 2bq + 2H2O		198.71	200.85	200.83
69 7ta = 3anth + 4bq + 4H2O		465.25	471.08	470.71
70 2anth + 2fo = 9en + 2H2O		183.15	185.22	183.93
71 ta + 2en = anth	2.0	9.72	10.15	9.86
72 9ta + 4fo = 5anth + 4H2O		452.08	458.06	456.64
73 br = per + H2O		81.91	82.72	82.29
74 mag = per + CO2	2.0	117.05	118.65	117.55
75 ta + 5mag = 4fo + 5CO2 + H2O		560.20	569.58	560.73
76 br + chr = 2fo + 3H2O		213.54	215.54	214.45
77 5chr = ta + 6fo + 9H2O	2.0	688.18	695.59	687.85
78 5chr = ta + 6fo + 9H2O	2.0	684.33	689.82	687.85
79 5chr = ta + 6fo + 9H2O	2.0	678.79	687.40	687.85
80 en + 2mag = 2fo + 2CO2	1.3	179.50	182.59	183.56
81 dol = cc + per + CO2	1.5	122.34	124.24	123.05
82 dol + 2q = di + 2CO2		158.66	161.47	160.16
83 5dol + 4ta = 6fo + 5di + 4H2O + 10CO2		1253.81	1279.58	1275.32
84 5dol + 8q + H2O = tr + 3cc + 7CO2		470.84	481.10	476.48
85 di + 3dol = 2fo + 4cc + 2CO2		210.11	214.56	215.50
86 2tr + 2fo = 5en + 4di + 2H2O		217.43	219.58	217.57
87 2dol + ta + 4q = tr + 4CO2		311.31	317.94	313.37
88 3dol + 4q + H2O = ta + 3cc + 3CO2		160.84	165.18	163.12
89 tr + 3cc + 2q = 5di + 3CO2 + H2O		326.23	331.90	324.33

calc	σ	uH	d/s	h(i)	ack	miss	Ref
31.18	1.03	0.51	1.9	0.36			Hays 67
50.32	0.88	1.45	1.9	0.02		-1.55	Gasparik 84
96.74	1.44	1.66	1.9	0.07			Shmulovich 74
50.87	0.83	1.03	1.7	0.08		1.67	Shmulovich 74
96.74	1.44	1.73	2.0	0.06			Hoschek 74
50.87	0.83	1.02	2.4	0.04		5.27	Hoschek 74
30.95	0.79	0.70	2.2	0.35		0.29	Chatterjee *et al.* 84
91.36	0.25	0.40	0.1	0.23			Chatterjee 74
91.36	0.25	0.40	0.8	0.06			Storre & Nitsch 74
82.57	0.21	0.34	-0.1	0.06			Storre & Nitsch 74
04.56	0.75	0.73	-0.1	0.63		-0.05	Jenkins 84
86.62	0.23	0.40	-0.9	0.05		1.97	Nitsch *et al.* 81
82.57	0.21	0.33	0.4	0.06			Nitsch *et al.* 81
51.71	0.69	0.82	2.2	0.20			Crawford & Fyfe 65
50.26	3.40	2.55	0.7	0.26			Nitsch 74
81.12	2.72	1.84	1.0	0.32			Newton & Kennedy 63, CJL 84
30.71	1.47	0.56	-0.1	1.00			Connolly & kerrick 85
34.74	0.21	0.16	0.8	1.00			Goldsmith & Newton 77
23.89	1.17	0.53	-0.9	0.71			Zharikov & Shmulovich 69
38.51	1.22	0.57	0.6	0.67			Zharikov & Shmulovich 69
16.06	23.26	6.71	2.0	1.00			Zharikov & Shmulovich 69
03.66	0.47	0.92	-0.5	0.15			Chernosky 76, CDC 85
20.56	0.37	0.97	0.4	0.09			Chernosky 76, CDC 85, S 71
17.09	0.37	0.66	0.5	0.19		1.80	Chernosky *et al.* 85
00.83	0.53	0.71	0.7	0.32			Chernosky & Autio 79
70.71	1.05	1.94	0.5	0.17			Chernosky & Autio 79
83.93	0.59	0.69	1.5	0.44			Chernosky *et al.* 85
9.86	0.22	0.11	1.9	0.34			Chernosky *et al.* 85
56.64	1.53	2.00	1.0	0.35			Chernosky *et al.* 85
82.29	0.33	0.27	-0.5	0.90			BE 63, IHW 77, SKB 82
17.55	0.70	0.53	0.9	0.25			Harker & Tuttle 55, GH 62
60.73	2.60	3.13	1.0	0.41			Greenwood 67
14.45	0.66	0.67	1.2	0.58			Johannes 68, Kitahara *et al.* 66
87.85	2.93	2.47	-1.4	0.21		-0.11	Chernosky 82
87.85	2.93	1.83	0.7	0.38			Kitahara *et al.* 66
87.85	2.93	2.36	1.8	0.15		0.15	Chernosky 73
83.56	1.04	1.03	1.3	0.36		0.93	Johannes 69
23.05	0.61	0.63	-3.5	0.25	1		Goldsmith 80
60.16	0.47	0.94	1.1	0.15			EK 81, JK 81, SKW 75
75.32	2.91	6.73	1.9	0.07			Skippen 71
76.48	1.63	3.42	0.3	0.13	1		Eggert & Kerrick 81, SKW 75
15.50	1.01	1.48	0.3	0.27	1	0.3	Kase & Metz 80
17.57	0.50	0.72	0.6	0.29			Jenkins 83
13.37	0.95	2.21	1.0	0.11			Eggert & Kerrick 81
63.12	0.93	1.45	0.4	0.24	1		EK 81, MP 71, GG 70
24.33	1.22	1.89	0.6	0.24		-1.56	Slaughter *et al.* 75

Table 5. (*Continued.*)

	Reaction	rfac	low	high	calc
90	tr + 11dol = 8fo + 13cc + 9CO2 + H2O		1012.20	1030.72	1026.15
91	3tr + 5cc = 11di + 2fo + 5CO2 + 3H2O		700.10	715.00	708.00
92	2tr = 3en + 4di + 2bq + 2H2O		234.06	237.27	234.48
93	2tr = 3en + 4di + 2bq + 2H2O	1.5	234.53	237.23	234.48
94	2tr = 3en + 4di + 2bq + 2H2O		234.94	237.23	234.48
95	2di + ta = tr		-6.94	-6.58	-6.96
96	3en + 2cor = 2py		51.19	53.05	52.96
97	fo + py = sp + 2en		-28.01	-26.39	-27.15
98	2py + 2bq = 3en + 2sill	2.0	-57.83	-55.31	-56.71
99	en + sp = mgts + fo		28.24	29.36	28.48
100	en + mgts = py		-1.56	-0.47	-1.33
101	clin = en + fo + sp + 4H2O		386.98	390.89	387.19
102	clin = en + fo + sp + 4H2O		386.81	390.50	387.19
103	clin + 2cor = py + 2sp + 4H2O	3.0	410.35	416.32	413.00
104	ames = en + 2sp + 4H2O		382.22	385.50	382.28
105	ames + fo = clin + sp		-5.41	-4.61	-4.91
106	clin + 2dol = 3fo + 2cc + sp + 4H2O + 2CO2		577.90	589.23	581.74
107	3clin + 2cc = 2di + 5fo + 3sp + 2CO2 + 12H2O		1295.46	1318.19	1314.23
108	clin + 2mag = 3fo + sp + 2CO2 + 4H2O		567.21	575.25	570.75
109	3clin + 14q = 3ky + 5ta + 7H2O	2.5	540.29	545.18	554.15
110	5en + 2sp = 5fo + crd	1.5	27.02	30.69	28.24
111	2clin + 3en = 7fo + crd + 8H2O	2.0	793.66	803.61	802.63
112	5clin + crd = 10en + 7sp + 20H2O	2.0	1882.13	1901.47	1907.72
113	5clin = 10fo + 3sp + crd + 20H2O	2.0	1955.74	1978.43	1964.21
114	6clin + 29q = 8ta + 3crd + 16H2O	3.0	1376.16	1393.03	1398.40
115	5en + 2sp = crd + 5fo	2.0	25.80	29.09	28.24
116	en + 3sill = crd + cor	2.0	7.43	10.14	7.17
117	2ta + 6sill + q = 3crd + 2H2O	3.0	230.35	238.99	238.17
118	2clin + 8ky + 11q = 5crd + 8H2O	2.0	851.70	868.24	852.93
119	2clin + 8and + 11q = 5crd + 8H2O	2.0	819.23	831.91	820.47
120	2clin + 19and = 5crd + 11cor + 8H2O	2.0	862.96	876.08	872.60
121	2clin + 19sill = 5crd + 11cor + 8H2O	2.0	776.67	789.55	785.25
122	2clin + 19ky = 5crd + 11cor + 8H2O	2.0	943.46	961.87	949.69
123	3mctd = py + 2cor + 3H2O		312.60	315.37	313.64
124	8mctd + 3cor + 7ky = 2mst + 4H2O		450.92	456.75	453.84
125	3mcar + q = ta + 3ky + 5H2O		400.75	404.61	404.96
126	14mcar = clin + 13ky + 3ta + 21H2O		1696.59	1713.38	1705.11
127	5mcar = clin + 4ky + 3q + 6H2O		490.31	495.82	490.22
128	2hb + 4fo = 5en + 4di + 2sp + 2H2O	2.0	187.64	191.83	189.74
129	3tats + 2q = 2ta + 3sill + H2O	2.0	16.96	18.68	16.83
130	29tats = 12crd + 3ta + 5clin + 6H2O	2.0	107.95	135.75	148.51
131	2wo + 2mont = di + merw	1.5	26.53	27.63	27.14
132	wo + mont = ak	1.5	20.87	21.16	21.14
133	di + merw = 2ak	1.5	14.36	15.58	15.15
134	di + 3mont = fo + 2ak	1.5	54.50	55.20	54.65
135	di + cc = ak + CO2		152.36	154.30	152.06
136	ak + fo + cc = 3mont + CO2	1.5	96.16	97.56	97.41

calc	σ	uH	d/s	h(i)	ack	miss	Ref
26.15	3.53	6.17	1.3	0.19	1		Metz 76
08.00	2.25	3.80	2.0	0.12			Chernosky & Berman 86
34.48	0.40	1.07	-0.6	0.09			Yin & Greenwood 83
34.48	0.40	0.90	0.9	0.05		-0.13	Boyd 59
34.48	0.40	0.76	-0.1	0.17		-1.13	Jenkins personal communication
-6.96	0.14	0.08	2.4	0.83		-0.13	Holland unpublished
52.96	0.71	0.62	0.5	0.76	2		Gasparik & Newton 84
27.15	0.44	0.54	0.2	0.39	2		Danckwerth & Newton 78, GN 84
56.71	0.78	0.84	0.8	0.13	2		Perkins 83
28.48	0.41	0.37	-0.5	0.70	2		Gasparik & Newton 84
-1.33	0.40	0.37	-1.3	0.71	2		Perkins *et al.* 81
87.19	0.70	1.23	1.6	0.17	2,3		Fawcett & Yoder 66
87.19	0.70	1.23	0.0	0.19	2,3		Jenkins 81, JC 86
13.00	1.11	1.02	2.9	0.02	3		Ackermand *et al.* 75
82.28	0.74	1.09	0.9	0.27	2,3		Jenkins 81
-4.91	0.34	0.27	-0.1	0.96	3		Jenkins 81
81.74	1.02	2.90	2.0	0.04	1,3		Chernosky & Berman 86
14.23	2.42	5.80	2.0	0.06	1,3		Chernosky & Berman 86
70.75	1.23	2.68	0.9	0.12	3		Chernosky & Berman 86
54.15	2.78	1.63	-0.2	0.28	3,4	3.22	Mirwald *et al.* 81
28.24	1.27	1.22	0.7	0.28	2		Herzberg 83
02.63	1.80	3.31	0.3	0.04	2,3		Jenkins & Chernosky 86
07.72	3.82	6.45	0.0	0.05	2,3	1.64	Jenkins & Chernosky 86
54.21	3.60	7.56	-0.5	0.03	3		Chernosky 74
98.40	5.59	5.62	-0.1	0.06	3,4	0.96	Chernosky 78
28.24	1.27	1.10	0.9	0.20	2		Seifert 74
7.17	0.87	0.90	0.4	0.14	2	-0.30	Newton 72
38.17	2.56	2.88	0.4	0.05	4		Newton 72
52.93	4.30	5.52	0.6	0.09	3		Seifert & Schreyer 70
20.47	4.31	4.22	0.8	0.15	3		Seifert & Schreyer 70
72.60	4.77	4.38	0.4	0.18	3		Seifert 73
85.25	4.72	4.29	0.1	0.18	3		Seifert 73
49.69	4.64	6.14	-0.3	0.08	3		Seifert 73
13.64	1.06	0.92	1.3	0.78			Chopin & Schreyer 83
53.84	2.53	1.56	1.9	1.00			Schreyer 68
04.96	0.94	1.28	0.3	0.31	4	0.38	Chopin & Schreyer 83
05.11	4.19	5.60	0.7	0.33	3,4		Chopin & Schreyer 83
90.22	1.56	1.84	0.6	0.42	3	-0.06	Chopin & Schreyer 83
89.74	3.64	1.40	0.8	1.00	5		Jenkins 83
16.83	1.33	0.57	-0.4	0.79	4	-0.10	Newton 72
48.51	15.29	9.27	-0.1	0.40	3,4	0.83	Fawcett & Yoder 66
27.14	0.50	0.25	2.2	0.49			Yoder 68
21.14	0.17	0.10	0.4	0.80			Yoder 68
15.15	0.52	0.41	0.5	0.43			Yoder 68
54.65	0.40	0.24	-0.6	0.75			Yoder 68, Walter 63
52.06	0.48	0.65	0.8	0.32	1	-0.65	Walter 63
97.41	0.55	0.46	0.5	0.37	1		Walter 63

Table 5. (*Continued.*)

Reaction	rfac	low	high	calc
137 fo + di + 2cc = 3mont + 2CO2	1.5	248.27	252.12	249.46
138 spu + 2mont = 2merw + cc	2.0	53.27	53.94	53.71
139 25pump = 29cz + 14gr + 5clin + 6q + 53H2O	3.0	3647.30	3693.24	3670.37
140 2vsv + 6q = 11gr + 4di + wo + 9H2O	2.5	469.97	473.46	471.73
141 kals + san = 2lc		31.62	32.52	32.12
142 san + fo = 1c + en	3.0	21.11	21.92	20.82
143 kals + 2en = san + 2fo		-10.20	-8.53	-9.52
144 5phl + 6cc + 24q = 3tr + 5san + 6CO2 + 2H2O	2.0	600.69	620.00	617.20
145 3dol + san + H2O = phl + 3cc + 3CO2		164.03	168.07	162.45
146 5mu + 3clin = 5phl + 8ky + q + 12H2O	3.0	1030.78	1040.61	1032.00
147 3cel = phl + 2san + 3q + 2H2O	2.0	155.63	158.15	156.89
148 3mu + 2phl = 3east + 2san + 3q + 2H2O	2.0	221.50	227.67	224.58
149 2phl + 6q = 3en + 2san + 2H2O	2.0	222.96	226.40	218.43
150 mu + cc + 2q = san + an + CO2 + H2O		183.28	186.44	183.89
151 2zo + mu + 2q = 4an + san + 2H2O		215.55	219.96	221.94
152 4law + ab = 2zo + pa + 2q + 6H2O	3.0	402.43	408.83	397.16
153 4law + jd = 2zo + pa + q + 6H2O	3.0	399.06	405.05	400.04
154 2parg = 3di + 2fo + 2ne + sp + an + 2H2O	2.0	262.81	266.51	264.67
155 2ed + sp = 3di + 2ne + an + 4fo + 2H2O	2.0	247.45	251.49	249.47
156 2jd + ta = gl		-9.61	-7.89	-8.75
157 2naph + 3en = 2abh + 6fo + 2H2O	2.0	241.01	243.72	242.37
158 arag = cc		0.31	0.46	0.38
159 ru + cc + q = sph + CO2		72.69	73.98	73.34
160 2ilm = 2iron + 2ru + O2		569.34	576.47	577.00
161 2usp = 2ilm + 2iron + O2		544.79	551.50	548.14
162 alm + 3ru = 3ilm + sill + 2bq		-2.90	-1.65	-2.48
163 gr + 2alm = 3fa + 3an	2.0	33.34	36.82	39.36
164 fs = fa + q		-1.48	-1.33	-1.42
165 fs = fa + bq		0.21	0.41	0.32
166 2alm + gr + 6ru = 6ilm + 3an + 3q	2.0	2.61	8.29	12.32
167 2alm + gr + 6ru = 6ilm + 3an + 3bq	2.0	9.12	14.99	17.52
168 alm + 2sill = 3herc + 5bq	2.0	26.39	28.55	27.83
169 6hem = 4mt + O2		469.32	474.13	472.02
170 3bq + 2mt = 3fa + O2		518.50	524.64	522.50
171 alm + phl = py + ann		46.69	47.93	46.96
172 py + 3fcel = alm + 3cel	3.0	-32.82	-32.09	-32.46
173 6sid = 2mt + gph + 5CO2		364.05	372.16	367.95
174 2hed + en = fs + 2di		-12.52	-11.89	-12.20
175 2phl + 3fs = 3en + 2ann	3.0	19.49	20.59	21.29
176 tr + 5hed = ftr + 5di	2.0	-9.80	-6.39	-8.10
177 2grun + 2fa = 9fs + 2H2O	2.0	206.03	211.13	208.58
178 2cumm + 7fs = 2grun + 7en	3.0	12.23	17.38	14.81
179 7en + 2fath = 2anth + 7fs	3.0	29.25	34.38	31.82
180 5gl + 3ftr = 3tr + 5fgl	3.0	-13.86	-10.96	-12.39
181 jd + ep = acm + cz	3.0	6.01	7.16	6.58
182 gl + 2acm = mrb + 2jd	3.0	-15.53	-14.44	-14.98
183 5alm + 3clin = 5py + 3daph	3.0	231.58	262.34	235.05

calc	σ	uH	d/s	h(i)	ack	miss	Ref
249.46	0.96	1.11	1.7	0.15	1		Walter 63
53.71	0.57	0.22	-0.4	0.95			Walter 65
3670.37	59.80	15.31	-1.3	1.00	3		Schiffman & Liou 80
471.73	3.78	1.16	0.9	1.00			Hochella *et al.* 82
32.12	0.38	0.30	0.8	0.97			Lindsley 66, Scarfe *et al.* 66
20.82	0.38	0.14	3.0	0.13		-0.74	Luth 67
-9.52	0.69	0.17	5.0	0.90			Wendlandt & Eggler 80
617.20	5.59	3.42	2.8	0.11			Hewitt 75
162.45	1.16	1.35	0.3	0.44	1	-1.36	Puhan 78, Puhan & johannes 74
1032.00	5.70	3.28	0.7	0.20	1		Bird & Fawcett 73
156.89	2.19	0.84	-2.0	1.00	6,7		Velde 65, MS 87
224.58	5.36	1.20	2.6	1.00	6,7		Massonne & Schreyer 87
218.43	2.08	0.89	1.9	0.49		-2.17	Bohlen *et al.* 83
183.89	0.54	1.05	0.4	0.15			Hewitt 73
221.94	0.59	1.47	0.8	0.10		3.36	Johannes 80
397.16	2.76	1.73	1.9	0.11		-1.91	Heinrich & Althaus 80
400.04	2.73	2.00	-0.8	0.12			Heinrich & Althaus 80
264.67	3.22	1.24	0.3	1.00	8		Westrich & Holloway 81
249.47	3.51	1.35	0.0	1.00	9		Westrich & Holloway 81
-8.75	0.75	0.09	9.3	1.00			Carman & Gilbert 83
242.37	2.35	0.90	-1.0	1.00			Carman & Gilbert 83
0.38	0.06	0.05	1.6	1.00			Johannes & Puhan 71
73.34	0.56	0.43	0.7	1.00			Jacobs & Kerrick 81
577.00	1.58	2.38	0.4	0.26		0.33	Anovitz *et al.* 85
548.14	2.91	2.24	0.7	1.00			Anovitz *et al.* 85
-2.48	0.52	0.42	-1.2	0.91			Bohlen *et al.* 83
39.36	1.73	1.16	-2.2	0.33	10	1.47	Bohlen *et al.* 83
-1.42	0.05	0.05	-0.8	0.64			Bohlen *et al.* 80
0.32	0.05	0.07	0.1	0.38			Bohlen *et al.* 80
12.32	1.30	1.89	0.6	0.07	10	3.11	Bohlen & Liotta 86
17.52	1.30	1.96	-0.6	0.06	10	1.95	Bohlen & Liotta 86
27.83	1.63	0.72	0.0	0.76	11		Bohlen *et al.* 86
472.02	2.07	1.60	-2.0	0.99			Meyers & Eugster 83
522.50	2.56	2.05	-2.6	0.92			Meyers & Eugster 83
46.96	0.52	0.42	-6.4	0.91	12		Ferry & Spear 78
-32.46	0.95	0.24	-4.9	1.00	12		Green & Hellman 82
367.95	3.44	2.70	0.8	0.25			Weidner 72
-12.20	0.27	0.21	-0.5	1.00	12		Lindsley 83
21.29	1.31	0.37	-19.5	0.84	12	0.53	Fonarev & Konilov 86
-8.10	2.96	1.14	-0.2	1.00	13		Robinson *et al.* 82
208.58	4.42	1.70	0.7	1.00	14		Fonarev & Korolkov 80
14.81	6.70	1.71	0.4	1.00	13		Butler 69
31.82	6.68	1.71	0.3	1.00	13		Robinson *et al.* 82
-12.39	3.77	0.96	-0.6	1.00	13		Robinson *et al.* 82
6.58	1.50	0.23	2.5	1.00	15		Nishiyama *et al.* 86
-14.98	1.41	0.36	-1.9	1.00	15		Sandrone *et al.* 86
235.05	3.23	1.90	8.1	0.01	13		Powell 85 + unpublished

Table 5. *(Continued.)*

	Reaction	xfac	low	high	calc	σ	uf	d/s	h(I)	ack	miss	Ref
184	5phl + 3daph = 5ann + 3clin	3.0	-0.97	0.53	-0.24	1.95	0.50	1.5	1.00	13		Powell 85 + unpublished
185	alm + 3mctd = py + 3fctd	2.0	22.55	24.53	24.25	1.27	0.66	-0.5	0.55	13		Chinner & Dixon 74, Miller 86
186	3mctd + fta = 3fctd + ta	2.0	-40.36	-38.62	-39.49	1.51	0.58	-9.5	1.00	13		Chinner & Dixon 74, M86, CM 84
187	fcar + mctd = mcar + fctd	3.0	-9.60	-8.91	-9.26	0.90	0.23	-3.3	1.00	13		Seidel & Okrusch 77, Seidel 81
188	3bq + 2hem + 3gr = 2andr + 3an	3.0	64.63	66.82	65.75	2.63	0.73	0.9	0.85	14		Liou 73
189	2ep = gr + an + hem + bq + H2O	3.0	78.94	80.26	79.63	1.24	0.44	0.7	0.52	14		Liou 73
190	6ep = 2andr + 6an + hem + 3H2O	2.0	302.11	307.34	304.65	3.59	1.74	-2.0	0.63	14		Liou 73
191	2hesc + 5bq = fcrd	3.0	-4.21	-2.89	-3.09	1.27	0.44	0.5	0.55	11		Richardson 68, HL 77
192	2alm + 4sill + 5bq = 3fcrd	3.0	42.43	46.06	46.39	3.51	1.21	-4.6	0.55		0.09	Richardson 68, HL 77
193	6fst + 25q = 8alm + 46ky + 12H2O	3.0	805.94	810.43	811.21	3.89	1.50	-1.3	0.44		0.20	Rao & Johannes 79
194	6fst + 25q = 8alm + 46ky + 12H2O	3.0	813.38	817.81	811.21	3.89	1.48	0.1	0.45		-0.56	Ganguly 72
195	2fst + 15bq = 4fcrd + 10sill + 4H2O	3.0	462.45	471.86	450.52	5.01	2.62	1.8	0.17		-2.38	Richardson 68
196	23fctd + 7q = 2fst + 5alm + 19H2O	3.0	1796.04	1815.22	1813.38	9.01	6.39	1.0	0.13			Rao & Johannes 79
197	8fctd + 10ky = 2fst + 3q + 4H2O	3.0	449.60	455.44	454.39	3.23	1.95	0.6	0.18			Rao & Johannes 79
198	3fctd = alm + 2cor + 3H2O	2.0	284.17	287.03	289.39	1.19	0.95	0.8	0.23		1.99	Ganguly 69
199	6fst + 25q = 8alm + 46sill + 12H2O	2.0	1197.33	1212.53	1209.35	6.36	5.07	0.8	0.23	14		Dutrow & Holdaway 86
200	8fctd + 10sill = 2fst + 3q + 4H2O	3.0	375.14	380.44	367.84	3.35	1.40	1.9	0.24		-2.18	Richardson 68
201	2deer = 9fs + 6mt + 6q + 10H2O	3.0	613.73	620.62	617.18	8.97	2.30	-0.3	1.00			Latard & Schreyer 81
202	pxmn = rhod		1.22	1.26	1.24	0.02	0.01	2.4	1.00			Maresch & Mottana 76
203	rhc + q = pxmn + CO2		86.12	87.74	86.93	0.70	0.54	-0.2	1.00			Peters 71
204	rhc = mang + CO2		111.83	113.47	112.65	0.71	0.55	1.1	1.00			Huebner 69
205	pxmn + rhc = teph + CO2		86.13	87.63	86.88	0.65	0.50	1.4	1.00			Huebner & Sugster 68
206	fdol + mag = dol + sid	3.0	-5.64	-4.37	-5.12	1.35	0.23	2.8	0.64	13		Anovitz & Essene 87
207	fdol + mag = dol + sid	3.0	-6.21	-2.96	-5.12	1.35	0.26	6.3	0.55	12		Rosenberg 67
208	en + 2fdol = 2dol + fs	3.0	-14.83	-10.63	-11.64	2.98	0.47	4.5	0.32	13		Klein 78

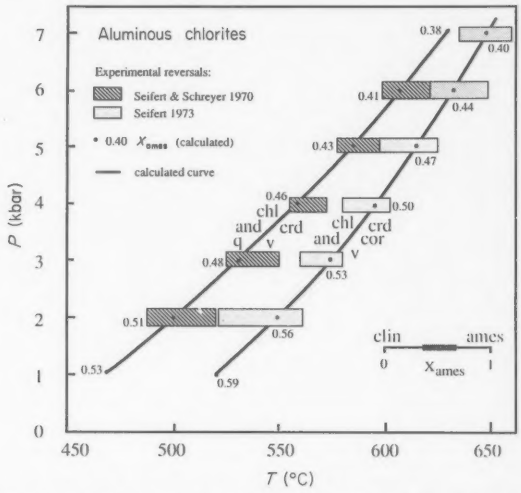

Fig. 2. Chlorite reactions in $MgO–Al_2O_3–SiO_2–H_2O$ showing the calculated compositions of chlorites along the univariant curves. X_{ames} in this diagram represents the mole fraction of amesite along the clinochlore ($X_{ames} = 0$) to amesite ($X_{ames} = 1$) solid solution. H_2O in cordierites was accommodated through the model of Kurepin (1985).

readers' comments and suggestions for further improvement in this (or any other) aspect of the dataset.

In the data extraction process we were forced to make some assumptions concerning the mixing properties in the tschermak substitutions. In this first attempt we have opted for the simplest defensible approach and used ideal mixing-on-sites to model the solid solutions. The formulae on which these models are based are given in Table 1 and activity expressions for the Mg end-members are given below as examples.

micas	mu	$4(X_{K,A})(X_{v,m1})(X_{Al,m2})^2[X_{Al,t2}][X_{Si,t2}]$
	cel	$4(X_{K,A})(X_{v,m1})(X_{Mg,m2})(X_{Al,m2})[X_{Si,t2}]^2$
	phl	$4(X_{K,A})(X_{Mg,m1})(X_{Mg,m2})^2[X_{Al,t2}][X_{Si,t2}]$
	east	$4(X_{K,A})(X_{Mg,m1})(X_{Mg,m2})(X_{Al,m2})[X_{Al,t2}]^2$
talc	ta	$(X_{Mg,m1})^2(X_{Mg,m2})[X_{Si,t2}]^2$
	tats	$4(X_{Mg,m1})^2(X_{Al,m2})[X_{Al,t2}][X_{Si,t2}]$
chlorite	clin	$16(X_{Mg,m1})^4(X_{Mg,m2})(X_{Al,m2})[X_{Al,t2}][X_{Si,t2}]$
	ames	$(X_{Mg,m1})^4(X_{Al,m2})^2[X_{Al,t2}]^2$
amphibole	tr	$(X_{v,A})(X_{Ca,m4})^2(X_{Mg,m13})^3(X_{Mg,m2})^2[X_{Si,t2}]^4$
	hb	$37.9(X_{v,A})(X_{Ca,m4})^2(X_{Mg,m13})^3(X_{Mg,m2})(X_{Al,m2})$ $[X_{Al,t2}][X_{Si,t2}]^3$

The activities of the Fe end-members can be found simply by replacing Mg with Fe in the above expressions. For practical applications these activity models should be adhered to, at least for the Tschermak substitutions. Of course, non-ideality in K–Na–Ca mixing or in Ca–Fe–Mg mixing may be added to the above ideal expressions, if desired. A computer program RECALC, available with THERMOCALC, makes such calculations automatic for mineral microprobe data and also propagates typical analytical uncertainties onto the final calculated site distributions and activities.

Table 6. Experiments not used in the regression. Symbols as for Table 5. Ref: JK 81, Jacobs & Kerrick,

	Reaction	rfac	low	high	calc
1	2dia = cor + H2O	2.0	82.04	83.08	81.73
2	pyhl = cor + 4q + H2O		79.18	81.24	80.21
3	pyhl = and + 3q + H2O		78.26	79.27	75.47
4	and = sill		4.16	4.21	4.60
5	and = sill		4.67	4.78	4.60
6	cc + bq = wo + CO2		91.73	93.14	90.19
7	gr + 2ky + bq = 3an		42.12	46.16	39.79
8	wo + cc + an = gr + CO2	2.0	44.29	45.28	41.85
9	2an + 3cc = geh + gr + 3CO2	2.0	284.31	294.48	292.72
10	ma + q = an + and + H2O	2.0	83.68	86.49	86.62
11	4law + 2q = 2zo + pyhl + 6H2O	2.0	403.24	422.37	409.71
12	12law = 6zo + 2ky + pyhl + 20H2O	2.0	1370.48	1409.69	1371.94
13	pre = an + wo + H2O	2.0	88.82	90.10	92.16
14	ta + 3cc + 2q = 3di + H2O + 3CO2		309.60	321.42	317.37
15	5ta + 6cc + 4q = 3tr + 6CO2 + 2H2O		589.22	617.07	613.86
16	2clin = py + 3fo + sp + 8H2O	3.0	803.12	808.82	801.53
17	mu + clin + 2q = crd + phl + 4H2O	2.0	376.65	381.61	376.99
18	cc + q + and = an + CO2	3.0	87.09	88.99	83.59
19	cc + q + ky = an + CO2	3.0	88.86	91.11	87.65
20	ru + cc + q = sph + CO2	2.0	74.99	76.36	73.34
21	daph + q = alm + fa + 4H2O	3.0	363.26	367.47	345.35
22	daph = 2fa + q + herc + 4H2O	3.0	368.41	372.87	356.78
23	2fgl = 4abh + 3fa + q + 2H2O	3.0	236.17	241.20	254.85
24	sid + hem = mt + CO2	3.0	77.87	79.70	74.41
25	6sid = 2mt + gph + 5CO2	3.0	371.79	379.56	367.95
26	andr = 3pswo + hem	3.0	51.70	52.49	48.80
27	andr = 3wo + hem	3.0	37.04	38.10	39.63
28	2py + 3fs = 2alm + 3en	3.0	-72.10	-63.02	-72.64
29	2py + 3fs = 2alm + 3en	3.0	-63.36	-56.53	-72.64
30	2py + 3fa = 2alm + 3fo	2.0	-51.46	-48.92	-48.22
31	2andr + bq + 3fa = 4hed + 2wo + 2mt	3.0	36.58	38.14	-3.06
32	3andr + mt + 9bq = 9hed + 2O2	3.0	1032.63	1048.48	991.29
33	6fst + 25q = 8alm + 46sill + 12H2O	2.0	1250.40	1273.19	1209.35

Kerrick, 1981.

calc	σ	uH	d/s	miss	ack	Ref
31.73	1.23	0.34	-0.1	-0.26		Matsuhisa et al. 67
30.21	1.27	0.32	3.2			Chatterjee et al. 84
75.47	1.25	0.34	0.2	-2.23		Kerrick 68
4.60	0.15	0.02	-2.9	2.53		Holdaway 71, Kerrick & Heninger 84
4.60	0.15	0.02	2.7	-0.48		Richardson et al. 69
90.19	0.26	0.47	-1.5	-5.87		Greenwood 67, Harker & Tuttle 55
89.79	0.83	1.35	0.4	-2.79		Hays 67, Gasparik 84
41.85	0.41	0.17	2.9	-5.88		Hoschek 74
92.72	1.11	1.24	4.1			Hoschek 74
96.62	0.23	0.40	3.5	0.60		Storre & Nitsch 74
09.71	2.99	1.78	5.4			Nitsch 72
71.94	8.25	5.83	3.4			Nitsch 72
92.16	0.35	0.43	-1.2	5.92		Chatterjee et al. 84
17.37	1.22	1.75	3.4			Skippen 71
13.86	2.49	3.60	3.9			Slaughter et al. 75
01.53	1.41	1.90	-1.6	-1.12	3	Staudigel & Schreyer 77
76.99	1.47	1.65	-0.3		3,6,7	Seifert 70
83.59	0.49	0.63	-1.0	-7.16		Jacobs & Kerrick 81
87.65	0.48	0.75	-1.0	-2.52		Jacobs & Kerrick 81
73.34	0.56	0.46	-0.7	-2.97		Hunt & Kerrick 77, JK 81
45.35	1.28	1.41	-0.7	-14.02		Hsu 68
56.78	1.49	1.49	-1.7	-7.78	11	Hsu 68
64.85	4.49	1.68	-1.3	3.04		Hoffmann 72
74.41	0.67	0.61	-1.1	-5.18		French 71
57.95	3.44	2.59	-6.3	-1.12		French 71
18.80	1.43	0.26	-0.7	-2.03		Huckenholz & Yoder 71
89.63	1.43	0.35	-10.8	1.07		Huckenholz & Yoder 71
72.64	1.55	0.55	8.3	-0.34	12	Lee & Ganguly 88
72.64	1.55	0.55	6.2	-5.97	12	Kawasaki & Matsui 83
48.22	1.71	0.54	2.3	0.41	12	O'Neill & Wood 79
-3.06	3.40	0.52	1.4	-11.66		Liou 74
01.29	6.72	5.28	0.7	-6.15		Burton et al. 82
09.35	6.36	5.30	2.1	-6.45		Richardson 68

PROBLEMS OF INCOMPATIBILITY AND POORLY CONSTRAINED DATA

For most end-members, the dataset has thrown up few significant problems in the way of incompatibility with experiments or unreliability due to unknown order–disorder or other thermodynamic behaviour. However, certain problems remain and come under three categories.

In the first category come problems of experimental incompatibility and we find the situation much as described by Berman (1988); Tables 5 and 6 highlight experimental reversals which were unsatisfied by the dataset and most of these were not incorporated in the least squares fit (Table 6). The column 'miss' should be scanned for values greater than 2, implying incompatibility at the 2σ level (or a miss by about half a bracket width). Reaction 49 in Table 5, involving gehlenite appears to be an outlier and reaction 109 involving talc and kyanite misses the high-pressure brackets with too steep a slope – these problems were also found by Berman (1988, figs 9, 10 and 32). The phl + q breakdown reaction to en + san + H_2O falls some 25 °C too low but possible non-stoichiometry of phlogopite (Massonne & Schreyer 1987) or high-temperature disorder might be the reason; the remaining reactions in Table 5 with 'miss' > 2 are characterized by only minor inconsistencies of the order of 10 °C or less except for some reactions involving Fe cordierite and/or Fe staurolite. Fcrd remains a problem (as does fst) because of its unknown H_2O content and P–T dependence. Table 6 lists reactions not used either (1) because the brackets are too wide to offer meaningful constraints (d/s large), (2) because of irreconcilable inconsistency ('miss' $\gg$ 2), or (3) because of severe slope inconsistencies.

In the second category we include the tschermak exchange end-members (cel, fcel, east, sdph, ames, fame, hb, fhb, tats, ftat) for which compositional information is scanty. These end-members are offered in the dataset because we believe that they will prove quite reliable in practice, if used with the stipulated ideal mixing-on-sites activity models. Again, we would welcome feedback from users of the dataset so that data for such end-members can be improved further and refined. Also in this second category come other phases whose compositions as a function of P–T or assemblage are poorly known and include fcrd, mst, fst, parg, ed, me, vsv, herc and deer. Further work is definitely required on data for these end-members.

In the third category we include those end-members whose enthalpies were derived from Fe/Mg or Fe^{3+}/Al exchange reactions taken from natural rocks. These may be found listed in Table 5 and in more detail in Appendix A. Geologically reasonable temperatures and pressures were assigned (with generous uncertainty brackets) to these natural occurrences and they were treated as pseudo-experiments in the data extraction. This will become potentially a very fruitful approach as more low-variance, well-equilibrated rocks become better characterized in terms of P, T, X_{H_2O} and thus provide reliable 'natural-lab' data. We put out a plea to petrologists to write to us with details of any well-characterized rocks which they feel hold promise for deriving or improving thermodynamic data.

ERRORS AND UNCERTAINTIES: THREE LEVELS OF RELIABILITY IN THE DATASET

As discussed previously in DS1, DS2 and DS3 attempts to determine uncertainties in thermodynamic calculations are crucial when using internally consistent datasets. It is frequently the case that the equilibrium of interest has not been experimentally determined and furthermore that it may involve thermodynamic data derived from disparate chemical subsystems. In such situations there is no intrinsic guarantee that an internally consistent dataset will provide calculated results with small uncertainties.

The magnitudes of enthalpy uncertainties given in Table 7 are not a good guide to the reliability of the data, because of the high correlations which exist among many phases. It is only when error propagation is performed, using the correlated uncertainties, that the magnitude of the error in a reaction enthalpy (and hence the error in P–T) can be determined. This is where the least squares method offers its most powerful advantage over linear programming; while it is possible to determine a set of uncorrelated errors from a linear programming analysis, ignoring the correlations means that no reliable estimates of error are possible as the following simple example shows: the error on the reaction jd + q = abh has a standard error, derived from correlated data, of $\sigma = 0.37$ kJ (Table 5, column 5), whereas the standard error calculated by ignoring the correlations is $\sigma = 5.24$ kJ [from Table 7: $\sigma^2 = (3.62)^2 + (3.72)^2 + (0.74)^2$]. In this example, error propagation using uncorrelated errors would overestimate the uncertainty by a factor of 14. In some cases the correlations work to cancel errors, while in others they work to amplify them. As explained in DS2 (p. 346), these correlations come about largely from the structure of the data themselves, from the stoichiometries of the reactions which specify linear combinations of enthalpies of formation, and are therefore an *integral and unavoidable* part of any internally consistent dataset. They are impossible to ignore.

A major change in the dataset from that proposed in DS2 is that we now present our data at three reliability levels. Level 1 (Table 7a) includes most of the data in common with DS2 and is regarded as most reliable. In this category are phases with well determined thermodynamic properties, principally entropies and volumes, and for which there are high-quality experimental phase equilibrium data available. Level 2 (Table 7b) contains phases whose data are slightly less reliable for a number of reasons: they may have poorly known entropies due to an unknown degree of cation disorder, they may be based on only one experimentally determined reaction, or they may be based on a reaction for which there are two or more incompatible experimental determinations. Cordierite is included in this level because the incomplete knowledge of

Table 7. Thermodynamic properties of the end-members whose formulae can be found in Table 1. The first two columns are least squares results. σ_H is one standard deviation on the molar enthalpy (H); S is the molar entropy; V is the molar volume, a, b, c and d are molar heat capacity polynomial coefficients, where the heat capacity, $C_p = a + bT + cT^{-2} + dT^{-1/2}$, αV and βV are the coefficients of thermal expansion and compressibility, respectively, multiplied by molar volume, and T_c and S_{max} are the Landau parameters discussed in the text. The factors under S, b, αV and βV are those by which elements in the respective columns must be multiplied to yield values in units of kJ, K and kbar. Reliability levels 1, 2 and 3 are discussed in the text.

(a) Reliability level 1. Thermodynamic properties (units: kJ, K, kbar).

End-member	$\Delta_f H$	$\sigma(\Delta_f H)$	S (x 10^{-3})	V	a	b (x 10^{-5})	c	d	αV (x 10^{-5})	βV (x 10^{-3})	T_c	S_{max} (x 10^{-3})
ab	-3937.86	3.72	207.40	10.007	0.4520	-1.3364	-1275.9	-3.9536	27.0	16.0	950	15.0
abh	-3929.13	3.71	220.00	10.043	0.4520	-1.3364	-1275.9	-3.9536	27.0	16.0		
ak	-3862.36	2.61	212.00	9.254	0.3854	0.3209	-247.5	-2.8899	28.0	6.2		
alm	-5267.85	3.20	342.00	11.511	0.7230	-2.6775	-1992.1	-6.0436	28.3	6.6		
an	-4232.74	1.98	199.30	10.079	0.3914	1.2556	-3036.2	-2.5832	14.3	13.0		
and	-2591.27	1.24	91.40	5.153	0.2904	-1.0520	-1109.0	-2.6280	12.7	2.8		
anth	-12064.14	7.85	537.00	26.540	1.2773	2.5825	-9704.6	-9.0747	74.0	33.0		
arag	-1208.16	1.11	88.00	3.415	0.0842	4.2844	-1397.5	0	8.3	5.3		
bq	-909.07	0.74	43.54	2.367	0.0979	-0.3350	-636.2	-0.7740	0	2.6		
br	-925.50	0.57	63.00	2.463	0.1584	-0.4076	-1052.3	-1.1713	7.0	2.6		
cats	-3305.64	1.61	138.00	6.356	0.3476	-0.6974	-1781.6	-2.7575	16.6	5.3		
cc	-1207.77	1.11	91.70	3.689	0.1847	-0.1226	513.9	-1.8486	9.0	5.3		
chr	-4358.11	2.80	221.30	10.746	0.6247	-2.0770	-1721.8	-5.6194	30.0	20.0		
coe	-908.17	0.74	39.00	2.064	0.1087	-0.4387	0	-1.0725	2.2	2.0		
cor	-1675.73	1.08	50.90	2.558	0.1574	0.0719	-1896.9	-0.9880	6.4	0.9		
di	-3200.15	1.90	142.70	6.619	0.3145	0.0041	-2745.9	-2.0201	22.0	5.5		
dia	-999.63	0.81	35.31	1.776	0.0515	5.4503	-1276.6	0	5.3	1.1		
diam	2.18	0.04	2.38	0.342	0.0243	0.6272	-377.4	-0.2734	0.3	0.1		
dol	-2325.72	1.26	155.20	6.434	0.3581	-0.5581	0	-3.4347	24.4	6.6		
en	-3089.38	2.08	132.50	6.262	0.3562	-0.2990	-596.9	-3.1853	18.0	4.6		
fa	-1478.80	1.63	151.00	4.630	0.0599	7.0620	-5743.7	2.0121	14.1	4.0		
fo	-2171.87	1.62	94.10	4.366	0.2349	0.1069	-542.9	-1.9064	16.0	3.2		
fs	-2388.19	2.04	192.00	6.592	0.3574	-0.2756	-711.1	-2.9926	24.0	5.8		
gph	-0.00	0.00	5.74	0.530	0.0510	-0.4428	488.6	-0.8055	1.5	1.4		
gr	-6638.30	3.91	256.00	12.535	0.7286	-4.0986	-3128.0	-6.0774	30.0	7.9		
hed	-2843.45	1.93	175.00	6.795	0.3104	1.2570	-1846.0	-2.0400	26.4	5.6		
hem	-822.54	1.41	87.40	3.027	0.1740	-0.3479	-1849.5	-0.8978	11.6	1.4	955	23.0
ilm	-1233.26	1.34	108.50	3.169	-0.0030	6.5050	-5105.7	2.4266	9.4	1.8		
iron	-0.00	0.00	27.28	0.709	0.0387	0.5944	415.7	-0.3726	2.9	0.4	1042	9.0
jd	-3029.94	3.62	133.50	6.040	0.3011	1.0143	-2239.3	-2.0551	17.0	4.5		
ksp	-3969.62	2.60	214.00	10.880	0.4488	-1.0075	-1007.3	-3.9731	20.6	20.0	725	16.0
ky	-2595.33	1.24	82.30	4.414	0.3039	-1.3390	-895.2	-2.9040	11.2	1.9		
law	-4868.07	2.08	230.00	10.132	0.9501	-11.3211	6645.6	-12.3180	25.0	9.0		
lime	-634.26	1.10	38.10	1.676	0.0524	0.3679	-752.0	-0.0500	6.7	1.7		
ma	-6241.64	2.62	265.00	12.964	0.7444	-1.6800	-2074.4	-6.7832	36.0	13.0		
mag	-1112.48	0.81	65.10	2.803	0.1947	-0.6081	287.4	-2.0738	10.6	3.0		
mang	-385.22	0.79	59.70	1.322	0.0598	0.3600	-31.4	-0.2826	5.4	0.8		
merw	-4539.72	3.59	253.10	9.847	0.4416	0.2228	-2002.9	-2.8882	35.0	7.9		
mont	-2250.36	1.43	108.10	5.148	0.2507	-1.0433	-797.2	-1.9961	19.0	4.4		
mt	-1115.81	2.10	146.10	4.452	0.2548	-0.6385	-2454.7	-1.4263	18.3	2.5	848	36.0
mu	-5981.63	2.81	289.00	14.083	0.7564	-1.9840	-2170.0	-6.9792	39.0	15.0		
pa	-5948.15	3.84	276.00	13.198	0.8030	-3.1580	217.0	-8.1510	42.0	17.0		
per	-601.41	0.48	26.90	1.125	0.0652	-0.1270	-461.9	-0.3872	4.6	0.7		
pswo	-1630.09	1.29	84.50	4.008	0.1071	1.7481	-2296.5	0	10.0	3.0		
pxmn	-1321.74	1.47	100.60	3.434	0.0990	1.9145	-3040.7	0.2745	8.3	3.1		
py	-6283.32	3.23	266.30	11.318	0.5450	2.0680	-8331.2	-2.2830	29.8	6.3		
pyhl	-5640.96	3.18	239.40	12.810	0.7845	-4.2948	1251.0	-8.4959	11.0	20.0		
q	-910.80	0.74	41.50	2.269	0.0979	-0.3350	-636.2	-0.7740	8.0	5.9		
rhc	-891.38	1.07	98.00	3.107	0.1497	1.8760	141.7	-1.3142	7.6	3.1		
rhod	-1320.51	1.47	102.50	3.471	0.0990	1.9145	-3040.7	0.2745	8.3	3.1		
ru	-944.75	1.09	50.30	1.882	0.0631	1.1307	-986.3	-0.0056	5.0	0.9		
san	-3959.06	2.58	230.00	10.892	0.4488	-1.0075	-1007.3	-3.9731	20.6	20.0		
sill	-2586.67	1.24	96.00	5.003	0.2261	1.4070	-2440.0	-1.3760	7.2	3.1		
sp	-2303.57	1.40	81.00	3.978	0.2229	0.6127	-1685.7	-1.5512	10.3	1.9		
ta	-5895.23	3.70	260.80	13.625	0.5343	3.7416	-8805.2	-2.1532	39.0	23.0		
teph	-1732.74	2.44	155.90	4.861	0.2613	-1.3780	0	-2.2177	14.8	4.2		
tr	-12302.50	7.06	550.00	27.270	1.2144	2.6528	-12362.0	-7.3885	84.5	36.0		
usp	-1507.33	1.97	168.90	4.682	-0.1026	14.2520	-9144.5	5.2707	19.2	2.6		
wo	-1633.15	1.29	81.70	3.993	0.1651	-0.1841	-793.3	-1.1998	9.6	3.6		
zo	-6896.18	3.27	295.00	13.558	0.6975	1.3263	-3794.1	-5.3179	34.5	8.0		
CH4	-74.81	0.59	186.26	0	0.1501	0.2062	3427.7	-2.6504	0	0		
CO	-110.53	0.29	197.67	0	0.0457	-0.0097	662.7	-0.4147	0	0		
CO2	-393.51	0.12	213.70	0	0.0878	-0.2644	706.4	-0.9989	0	0		
H2	0.00	0.00	130.70	0	0.0233	0.4627	0	0.0763	0	0		
H2O	-241.81	0.03	188.80	0	0.0401	0.8656	487.5	-0.2512	0	0		
O2	-0.00	0.00	205.20	0	0.0483	-0.0691	499.2	-0.4207	0	0		

Table 7. (*Continued.*)

(b) Reliability level 2. Thermodynamic properties (units: kJ, K, kbar).

End-member	$\Delta_f H$	$\sigma(\Delta_f H)$	S (x 10^{-3})	V	a	b (x 10^{-5})	c	d	αV (x 10^{-5})	βV (x 10^{-3})	T_c	S_{max} (x 10^{-3})
andr	-5761.60	4.31	316.40	13.204	0.8092	-7.0250	-678.9	-7.4030	32.0	8.3		
ann	-5149.32	3.61	414.00	15.432	0.8157	-3.4861	19.8	-7.4667	43.0	15.0		
clin	-8919.25	4.38	421.00	21.090	1.1618	1.0133	-7657.3	-9.6909	59.0	38.0		
crd	-9166.50	4.39	407.50	23.322	0.8213	4.3339	-8211.2	-5.0000	14.5	40.0		
cz	-6900.99	3.27	291.00	13.673	0.6975	1.3263	-3794.1	-5.3179	35.0	8.0		
czl	-6896.98	3.43	291.00	13.673	0.6975	1.3263	-3794.1	-5.3179	35.0	8.0		
di.o	-3192.79	3.93	148.50	6.425	0.3145	0.0041	-2745.9	-2.0201	22.0	5.5		
en.c	-3083.25	4.03	135.00	6.262	0.3562	-0.2990	-596.9	-3.1853	18.0	4.6		
ep	-6462.05	3.20	326.00	13.920	0.6979	-0.9993	-5105.3	-4.7101	35.0	8.0		
fctd	-3211.38	1.48	162.00	6.980	0.4846	-1.3808	-198.9	-4.7622	19.0	7.5		
fdol	-1969.30	1.97	185.60	6.572	0.4421	-4.7430	2037.0	-4.9310	16.0	8.2		
geh	-3977.26	2.50	212.00	9.024	0.4057	-0.7099	-1188.3	-3.1744	23.0	8.0		
gl	-11963.86	8.16	535.00	26.050	1.7175	-12.1070	7075.0	-19.2720	70.0	29.0		
hb	-12420.29	6.36	551.00	26.990	1.2296	2.5438	-12163.5	-7.7503	83.0	35.0		
herc	-1956.00	1.45	116.00	4.075	0.2380	0.6820	-903.1	-1.8627	9.4	2.1		
kals	-2114.50	3.09	134.00	6.040	0.2420	-0.4482	-895.8	-1.9358	20.0	10.0		
lc	-3020.72	2.72	202.20	9.117	0.3698	-1.6332	684.7	-3.6831	31.0	14.0	955	19.0
mcar	-4794.81	1.90	194.00	10.590	0.6678	-1.2559	-1167.1	-6.4400	31.0	19.0		
mctd	-3557.95	1.48	132.00	6.875	0.4644	-1.2654	-1147.2	-4.3410	20.0	5.9		
me	-13871.25	6.51	720.00	34.040	1.3160	6.4990	-8963.0	-8.9320	48.0	48.0		
mgts	-3192.61	1.51	127.00	5.890	0.3714	-0.4082	-398.4	-3.5471	17.0	4.3		
mst	-25118.49	11.14	890.00	44.260	2.8205	-5.9366	-13774.0	-24.1260	12.0	32.0		
ne	-2105.44	3.85	123.00	5.740	0.2727	-1.2398	0	-2.7631	26.0	11.5	467	10.0
phl	-6211.76	3.51	325.00	14.964	0.7703	-3.6939	-2328.9	-6.5316	39.0	24.5		
pre	-6199.86	3.09	292.80	14.026	0.7249	-1.3865	-2059.0	-6.3239	42.0	16.0		
rnk	-3721.07	8.48	197.20	9.651	0.6723	-0.2893	-2462.4	-2.1813	36.0	9.6		
sid	-761.18	0.91	95.50	2.938	0.2574	-4.6200	1523.0	-3.0819	7.2	2.9		
sph	-2596.48	1.77	129.20	5.565	0.1767	2.3852	-3990.5	0	14.0	3.3		
spu	-5840.20	5.72	330.00	14.697	0.6141	-0.3508	-2493.1	-4.1680	55.0	14.7		
ty	-6372.21	5.71	380.80	17.039	0.7417	-0.5345	-1434.6	-5.8785	64.0	17.0		

(c) Reliability level 3. Thermodynamic properties (units: kJ, K, kbar).

End-member	$\Delta_f H$	$\sigma(\Delta_f H)$	S (x 10^{-3})	V	a	b (x 10^{-5})	c	d	αV (x 10^{-5})	βV (x 10^{-3})	T_c	S_{max} (x 10^{-3})
acm	-2584.42	4.07	170.60	6.459	0.3502	0.4154	-453.0	-3.0229	18.0	4.8		
ames	-9046.04	3.96	400.00	20.920	1.1770	0.9041	-7458.7	-10.0530	58.0	38.0		
cel	-5834.27	2.89	297.00	13.960	0.7412	-1.8748	-2368.8	-6.6169	39.0	16.0		
cumm	-12075.73	8.79	542.00	26.470	1.2773	2.5825	-9704.6	-9.0747	74.0	33.0		
daph	-7148.44	4.50	559.00	21.340	1.2374	1.3594	-3743.0	-11.2500	59.0	38.0		
deer	-18344.32	15.53	1650.00	55.950	3.1644	-2.7883	-5039.1	-26.7210	168.0	56.0		
east	-6336.56	3.78	315.00	14.751	0.7855	-3.8031	-2130.3	-6.8937	38.0	24.0		
ed	-12580.53	6.78	599.00	27.090	1.2649	2.4090	-12560.0	-7.7040	84.0	30.0		
fame	-7629.39	4.43	513.00	21.120	1.2375	1.1810	-4417.3	-11.3003	58.0	38.0		
fath	-9625.86	8.34	729.00	27.870	1.3831	3.0669	-4224.7	-11.2576	79.0	32.0		
fcar	-4438.98	2.13	223.00	10.690	0.6748	-1.0092	-715.8	-6.5545	30.0	0.0		
fcel	-5484.96	2.91	328.00	14.000	0.7563	-1.9147	-1586.1	-6.9287	39.5	16.9		
fcrd	-8460.45	4.40	458.00	23.710	0.8515	4.4724	-6645.0	-5.6234	13.0	40.0		
fgl	-10901.10	8.35	624.00	26.590	1.7629	-11.8992	9423.7	-20.2071	81.0	31.0		
fhb	-10999.97	7.01	690.00	27.900	1.2900	2.8209	-9031.9	-8.9971	87.0	36.0		
fst	-23745.11	11.04	1030.00	44.880	2.8800	-5.6595	-10642.0	-25.3730	13.0	36.0		
fta	-4816.02	4.14	358.00	14.790	0.5797	3.9494	-6459.3	-3.0881	42.0	25.0		
ftat	-5276.36	3.52	323.80	14.067	0.5798	3.7709	-7042.7	-3.1386	41.0	25.0		
ftr	-10527.10	7.66	705.00	28.280	1.2900	2.9991	-8447.5	-8.9470	88.0	37.0		
grun	-9614.14	7.95	734.00	27.800	1.3831	3.0669	-4224.7	-11.2576	79.0	32.0		
mrb	-11087.79	9.11	602.00	27.130	1.7015	-11.5650	7021.6	-18.5336	73.0	30.0		
naph	-6173.64	4.46	315.00	14.450	0.7735	-4.0229	-2597.9	-6.5126	43.0	24.0		
parg	-12719.83	6.05	591.00	27.210	1.2802	2.2997	-12359.5	-8.0658	84.0	30.0		
pump	-14384.48	6.74	629.00	29.550	1.7208	-2.4928	-5998.7	-14.6203	88.0	18.0		
sdph	-5628.27	4.22	375.00	15.063	0.8158	-3.6645	-564.5	-7.5171	41.0	18.0		
tats	-5995.84	2.81	259.00	13.290	0.5495	3.6324	-8606.6	-2.5153	39.0	24.0		
vsv	-42319.11	24.21	1890.00	85.200	4.4880	-5.7952	-22269.3	-33.4780	239.0	48.0		

its hydration thermodynamics means that data for this phase may be improved later as our understanding increases. Because of the internal consistency of the dataset as a whole there is relatively little difference in reliability between level 2 and level 1 for practical purposes. Level 3 (Table 7c) is distinctly different in character, and includes many phases for which the thermodynamic data are to be regarded as preliminary. They are included in this level because they have been derived from natural partitioning data, because they have been derived using simplified ideal mixing solution models, because their compositions or entropies are poorly known, or because of incompatibilities in the experimental data.

We anticipate that data in level 1 will not change significantly as more experimental and thermodynamic data are accumulated. Level 2 data may be improved as further measurements and experiments are made, but changes are not expected to be extensive. Level 3 data are highly preliminary and may be subject to major changes in the future; some data in this category may well be very reliable, and we present level 3 data because it is only by testing such data and refining them in the future that progress can be made. We have also had some experience in using these data to calculate both conditions of formation in rocks as well as phase diagrams, with very encouraging results (see practical applications below).

EXAMPLE APPLICATIONS USING THE NEW DATASET

Aluminous chlorites and talcs

Figure 2 shows the results of calculations on two chlorite–andalusite breakdown reactions in the MgO–Al_2O_3–SiO_2–H_2O system, discussed briefly above. For each of these univariant reactions it is necessary to solve two non-linear equations, for temperature and chlorite composition, at any specified pressure. For the examples shown in Fig. 2 the relations are:

(a) Univariant reaction: andalusite + chlorite = cordierite + corundum + H_2O. The independent set of 2 reactions used is:

(1) 19 and + 2 clin = 5 crd + 11 cor + 8 H_2O.

(2) 8 and + ames = 2 crd + 6 cor + 4 H_2O.

(b) Univariant reaction: andalusite + chlorite + quartz = cordierite + H_2O. The independent set of 2 reactions

Table 8. Diagnostics of the fitted enthalpies; for details of diagnostics A, B and C see the text.
(a) ΔH_R change on doubling ΔH bracket, scaled to 'expected' $\sigma(\Delta H_R)$ using 0.15 kJ/atom, and using a cut-off of 0.25.

Reaction	End-member	Change
diam = gph	diam	0.65
cc = lime + CO_2	lime	0.53
ta + 5mag = 4 fo + 5 CO_2 + H_2O	mag	−0.26
en + 2 mag = 2 fo + 2 CO_2	mag	0.33
2 ilm = 2 iron + 2 ru + O_2	fa	0.31
	hem	0.39
	mt	0.29
	ilm	0.31

(b) [$\sigma(\Delta_f H$: enlarged ΔH_R bracket)/$\sigma(\Delta_f H) - 1$], using a cut-off of 0.05.

Reaction	End-member	Change
diam = gph	diam	0.40
2 dia = cor + H_2O	dia	0.14
spu + 4 wo = 3 rnk + CO_2	rnk	0.35
br = per + H_2O	br	0.11
25 pump = 29 cz + 14 gr + 5 clin + 6 q + 53 H_2O	pump	0.06
3 mu + 2 phl = 3 east + 2 san + 3 q + 2 H_2O	sdph	0.08
	east	0.10
2 usp = 2 ilm + 2 iron + O_2	usp	0.24
3 bq + 2 mt = 3 fa + O_2	fa	0.05
tr + 5 hed = ftr + 5 di	ftr	0.07
	fhb	0.05
2 cumm + 7 fs = 2 grun + 7 en	cumm	0.07
7 en + 2 fath = 2 anth + 7 fs	fath	0.08
jd + ep = acm + cz	acm	0.07
	mrb	0.05
3 mctd + fta = 3 fctd + ta	fta	0.06
fcar + mctd = mcar + fctd	fcar	0.08
rhc + q = pxmn + CO_2	rhod	0.11
	pxmn	0.11
rhc = mang + CO_2	rhod	0.11
	pxmn	0.11
	teph	0.16
	rhc	0.20

(c) $\Delta_f H$ change on moving ΔH_R bracket by 1/4 width, scaled to 'expected' $\sigma(\Delta_f H)$, using 0.15 kJ/atom, and using a cut-off of 0.25.

Reaction	End-member	Change
pyhl + 6 dia = 4 and + 4 H_2O	dia	0.31
2 dia = cor + H_2O	dia	0.49
2 jd = ne + abh	ne	−0.56
cc = lime + CO_2	lime	−0.28
spu + 4 wo = 3 rnk + CO_2	rnk	−2.48
mag = per + CO_2	mag	0.25
dol = cc + per + CO_2	fo	0.26
kals + 2 en = san + 2 fo	kals	0.36
3 mu + 2 phl = 3 east + 2 san + 3 q + 2 H_2O	east	−0.31
ru + cc + q = sph + CO_2	sph	−0.27
2 ilm = 2 iron + 2 ru + O_2	fs	0.25
	fa	0.38
	mt	0.45
	hem	0.41
	ilm	0.31
2 usp = 2 ilm + 2 iron + O_2	usp	0.80
alm + 2 sill = 3 herc + 5 bq	herc	−0.26
3 bq + 2 mt = 3 fa + O_2	fa	−0.30
tr + 5 hed = ftr + 5 di	ftr	−0.28
2 cumm + 7 fs = 2 grun + 7 en	cumm	0.31
dol + sid = fdol + mag	fdol	−0.28
7 en + 2 fath = 2 anth + 7 fs	fath	0.31
jd + ep = acm + cz	acm	−0.58
	mrb	−0.28
3 mctd + fta = 3 fctd + ta	fta	0.28
rhc + q = pxmn + CO_2	rhod	−0.54
	pxmn	−0.54
	teph	−0.38
rhc = mang + CO_2	rhod	0.55
	pxmn	0.55
	teph	0.78
	rhc	0.55
pxmn + rhc = teph + CO_2	teph	−0.36

used is:

(1) 8 and + 11 q + 2 clin = 5 crd + 8 H_2O

(2) 2 and + 6 q + ames = 2 crd + 4 H_2O.

Solution of the above equations at specified pressures, using THERMOCALC, yielded the temperatures and chlorite compositions for the univariant reactions in Fig. 2.

We have found that the chlorites coexisting with aluminosilicates or corundum at medium to low pressures are very aluminous, but at high pressures and lower temperatures the Al solubility decreases, and, in some assemblages at high pressures, the chlorite even becomes considerably less aluminous than clinochlore. It is not, however, necessary to introduce a new Al-free end-member, because the activities of both amesite and clinochlore are well-defined in the solid solution series $Mg_6Si_4O_{10}(OH)_8$–$Mg_4Al_2Si_2Al_2O_{10}(OH)_8$. The predicted alumina solubility in chlorites is in good agreement with the assemblages discussed by Jenkins (1983) in experimental studies and with natural whiteschist occurrences.

Since this phase of the study was completed, Massonne (1989) has provided new experimental data on the reactions (i) chlorite + quartz = talc + cordierite + H_2O and (ii) talc + kyanite + quartz = cordierite ± H_2O. Our thermodynamic data yield calculated curves for these two equilibria which pass through all Massonne's reversal brackets. Furthermore our calculated alumina contents of talc and chlorite are only slightly higher than Massonne's rather preliminary estimates. Massonne (1989) also restudied the reaction (iii) chlorite + quartz = kyanite + talc + H_2O and found that the Al content of talc decreased with increasing pressure along this reaction – exactly as we have also found by calculation. Thus the discrepancy between the calculations (our data as well as those of Berman, 1988) and the highest pressure brackets of Massonne on reaction (iii) cannot be ascribed to unusually high Al contents of talc, as suggested by Berman in his fig. 32f.

Solid solutions of chlorite, garnet and glaucophane in NFMASH

As an extension of the simple logic outlined above for the chlorite equilibria, we now examine a univariant reaction in NFMASH and its termination at an invariant point in NFASH. The reactions are plotted in Fig. 3, and Table 9 gives the calculated data for the univariant reaction:

garnet + paragonite + glaucophane

= chlorite + albite (quartz, H_2O in excess).

To determine the P–T location of this reaction requires the solution to five independent equilibria (non-linear relations of the form $\Delta G^\circ = \sum RT \ln a_i$) to determine (1) pressure of the reaction at the chosen temperature, (2) X_{Fe} in garnet, (3) X_{Fe} in glaucophane, (4) X_{Fe} in chlorite, and (5) the degree of tschermak substitution y(chl) in chlorite. The set of five reaction equilibria used to construct the

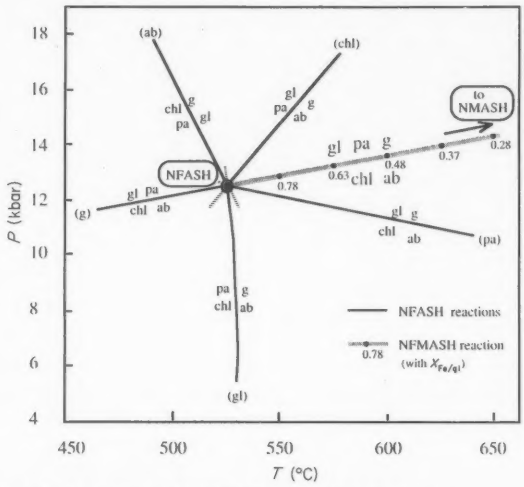

Fig. 3. An example of a calculated univariant reaction in NFMASH emanating from the NFASH invariant point involving phases garnet (g), glaucophane (gl), paragonite (pa), chlorite (chl), albite (ab), quartz (q) and H_2O. Details of the compositions of all phases along each reaction are given in Table 9.

univariant reaction in Fig. 3 is:

4 q + clin + ames = 3 py + 8 H_2O

13 ab + q + 3 clin = 3 pa + gl + 4 H_2O

pa + q + gl = 3 ab + py + H_2O

pa + q + fgl = 3 ab + alm + 2 H_2O

5 py + 3 daph = 5 alm + 3 clin.

As the reaction is traced away from its termination at the NFASH invaraint point, the compositions of garnet, chlorite, and glaucophane become more magnesian (Fig. 3 and Table 9). The alumina content of the chlorite along the univariant NFMASH reaction is approximately constant at a value just less than the (Fe, Mg) clinochlore composition; the situation for the various NFASH reactions is quite different, involving aluminous chlorites at low pressures along the gl-absent reaction to almost alumina-free compositions at higher temperatures on the pa-absent reaction (Table 9).

While the exact P–T location of this set of equilibria may be in some dispute because of the tenuous assumptions involved in extracting data for aluminous Fe-chlorites and Fe-glaucophane, this example illustrates the important principle that compositions in such solid solutions may vary considerably with pressure, temperature and assemblage. Any experimental studies aimed at determining univariant reactions in even such simple systems as these must take into account this variation – which may require experimental reversal of as many as four or more mineral-compositional variables, a truly daunting task at such low temperatures. We feel that methods such as these, where a set of end-member thermodynamic properties may be readily determined, hold the best promise for calibration of complex natural reactions where direct experiment becomes impossible.

Table 9. Reactions in NFMASH involving the phases garnet (g), glaucophane (gl), paragonite (pa), chlorite (chl), albite (ab), quartz (q) and H_2O. x(g) refers to the Fe/(Fe + Mg) ratio in garnet etc; y(chl) refers to the Al content in chlorite ($y = 0$ in Al-free chlorite, $y = 0.5$ in clinochlore and daphnite, and $y = 1$ in amesite and ferroamesite). Mixing-on-sites activities were used in the calculations.

(a) NFASH invariant point involving gl, g, chl, ab and pa (q, H_2O).

P(kbar)	T(°C)	y(chl)
12.5	523	0.433
sd 0.9	6	0.0413

Correlation between P and T: $\rho = -0.101$

(b) NFMASH reaction gl + g + pa = chl + ab (+q, H_2O).

T(°C)	P(kbar)	x(gl)	x(g)	x(chl)	y(chl)
530	12.7	0.946	0.993	0.948	0.402
540	12.8	0.859	0.978	0.863	0.409
550	12.9	0.780	0.963	0.786	0.415
560	13.0	0.709	0.945	0.716	0.421
570	13.1	0.644	0.926	0.652	0.427
580	13.2	0.585	0.904	0.594	0.433
590	13.4	0.531	0.881	0.540	0.439
600	13.5	0.481	0.855	0.490	0.444
610	13.7	0.435	0.827	0.444	0.450
620	13.8	0.392	0.796	0.401	0.455
630	13.9	0.353	0.763	0.361	0.460
640	14.1	0.316	0.727	0.324	0.464

(c) NFASH reactions about the above invariant point.

(i) Reaction involving the phases: gl, g, chl, ab (q, H_2O) [pa absent].

T(°C)	P(kbar)	y(chl)
540	12.0	0.366
550	11.7	0.332
560	11.5	0.301
570	11.3	0.273
580	11.2	0.249
590	11.0	0.227
600	10.9	0.207
610	10.8	0.190
620	10.8	0.174
630	10.7	0.160
640	10.7	0.147
650	10.6	0.135
660	10.6	0.125

(ii) Reaction involving the phases: gl, g, chl, pa (q, H_2O) [ab absent].

P(kbar)	T(°C)	y(chl)
13.0	520	0.429
14.0	515	0.421
15.0	508	0.413
16.0	502	0.405
17.0	495	0.397

(iii) Reaction involving the phases: gl, chl, ab, pa (q, H_2O) [g absent].

T(°C)	P(kbar)	y(chl)
350	10.6	0.294
370	10.8	0.314
390	11.0	0.332
410	11.2	0.350
430	11.4	0.366
450	11.6	0.382
470	11.8	0.397

(iv) Reaction involving the phases: gl, g, ab, pa (q, H_2O) [chl absent].

P(kbar)	T(°C)
13.0	530
14.0	544
15.0	557

(v) Reaction involving the phases: g, chl, ab, pa (q, H_2O) [gl absent].

P(kbar)	T(°C)	y(chl)
5.0	531	0.687
6.0	532	0.654
7.0	531	0.620
8.0	530	0.586
9.0	528	0.551
10.0	527	0.517
11.0	525	0.483
12.0	524	0.450

This example is drawn from the much larger study of Guiraud, Holland & Powell (1989) of equilibria in an NFMASH petrogenetic grid for blueschists and eclogites, with the NFASH invariant point here being $f2$ in that study. The reader should be cautioned against taking the pressures and temperatures for the NFMASH grid too literally because natural assemblages in metabasites contain additional cations such as Ca and Fe^{3+} which will greatly enhance the stability of the amphibole and garnet and thus reduce the pressures of the NFMASH univariant reaction discussed above.

We have also made progress in calibrating the pelite petrogenetic grid of Harte & Hudson (1979) in the KFMASH system, involving the phases staurolite, chloritoid, aluminosilicates, cordierite, biotite, phengite, garnet, chlorite and quartz, where Tschermak as well as Fe/Mg substitutions are considered, and present those conclusions elsewhere (Powell & Holland, 1989). The compositions of the pelite minerals (Fe/Mg ratios and Tschermak substitutions) and their variation with P, T and mineral assemblage are in close agreement with natural occurrences. Although it will be some time before such calculations become routinely reliable in complex natural systems, the success to date in some of the simpler cases which we have examined is very encouraging.

Further average pressure calculations for RP13

The Scottish Dalradian rock RP13, discussed in considerable detail elsewhere (Powell, 1985; Powell &

Table 10. Average pressure calculations for rock RP13.

(a) Phases and end-member activities.

Phase		Activity	$\sigma_{\ln a}$
muscovite			
mu	muscovite	0.682	0.018
cel	celadonite	0.034	0.399
biotite			
phl	phlogopite	0.0774	0.316
ann	annite	0.0140	0.519
east	eastonite	0.0450	0.372
chlorite			
clin	clinochlore	0.0580	0.345
ames	amesite	0.0270	0.419
daph	daphnite	0.0090	0.564
garnet			
gr	grossular	0.0157	0.505
py	pyrope	0.00098	0.730
alm	almandine	0.190	0.163
andr	andradite	0.00016	0.805
plagioclase			
an	anorthite	0.561	0.058
epidote			
cz	clinozoisite	0.650	0.037
ep	epidote	0.350	0.100
calcite			
cc	calcite	1.000	0.000
quartz			
q	quartz	1.000	0.000

(b) An independent set of reactions for RP13.

(1) $4\,cz + q = gr + 5\,an + 2\,H_2O$
(2) $2\,cz + CO_2 = 3\,an + cc + H_2O$
(3) $3\,py + 16\,cz = clin + ames + 4\,gr + 20\,an$
(4) $4\,clin + 44\,cz = 5\,ames + 14\,gr + 46\,an + 18\,H_2O$
(5) $5\,alm + 24\,cz + 3\,q = 3\,daph + 5\,gr + 33\,an$
(6) $8\,mu + 3\,cel + 6\,clin + 7\,gr = 11\,phl + 21\,an + 24\,H_2O$
(7) $3\,daph + 12\,andr + 33\,an = 7\,gr + 5\,alm + 24\,ep + 3\,q$
(8) $2\,mu + gr + py = cel + east + 3\,an$
(9) $phl + 3\,an = mu + gr + py$
(10) $ann + 3\,an = mu + gr + alm$

(c) calculated pressures for rP13 at 530 °C.

Reaction	P(530 °C)	σ	dP/dT	ln K
(1)	6.5	0.43	0.0290	−5.321
(2)	6.7	0.33	0.0160	−0.873
(3)	6.5	0.57	0.0117	−6.960
(4)	6.2	0.62	0.0282	−72.463
(5)	6.8	0.41	0.0167	−35.335
(6)	6.4	0.74	0.0403	19.083
(7)	9.2	1.15	0.0193	75.513
(8)	7.0	1.13	0.0114	3.631
(9)	6.8	0.94	0.0068	−7.172
(10)	8.0	0.73	0.0166	−0.195

(d) Average pressures for RP13.

For $X_{CO_2} = 0.25$ and $X_{H_2O} = 0.75$						
T(°C)	480	500	520	540	560	580
av P	5.3	5.9	6.6	7.1	7.7	8.3
σ	0.54	0.40	0.30	0.26	0.33	0.47
σ_{fit}	2.4	1.7	1.2	1.1	1.3	1.8
No fluid						
T(°C)	480	500	520	540	560	580
av P	6.3	6.7	7.0	7.3	7.6	7.9
σ	0.28	0.29	0.29	0.30	0.31	0.33
σ_{fit}	1.0	1.0	1.0	1.0	1.0	1.0

Holland, 1988), appears to be a remarkably well-equilibrated calc-pelite assemblage. The enlargement of the dataset since our earlier publications enables the average pressure to be determined from a much larger independent set of mineral equilibria (Powell & Holland, 1988; Holland, 1988), as well as providing a test of some of the newer mineral end-member data. The methods used need not be discussed again in detail here, except to say that the average pressure is defined as the optimum pressure, in the least squares sense, derived from the calculated individual pressures of the independent set of reactions weighted according to their correlated uncertainties.

In the earlier analysis (DS3) rock RP13 was characterized by four independent barometric reactions, whereas with the newer dataset it is now possible to determine ten independent constraints on the pressure of formation. It should be clear that, provided the data are of reasonable quality, there is considerable statistical advantage in increasing the number of independent pressure estimates, much as in conducting replicate experiments to reduce the uncertainties in experimental studies. Table 10 and Fig. 4 summarize the average pressure results for RP13. These pressures are in excellent agreement with the earlier study using the old dataset and even allow very good pressure estimates from the fluid-conserving reactions, thus avoiding any dependence on the assumed composition for the metamorphic fluid. In fact the results of this rock are so consistent that they allow determination of a unique optimum P and T simultaneously, as will be discussed in a further publication (R. Powell & T. J. B. Holland, unpublished data).

RESULTS AND DISCUSSION

The enthalpies of formation of the end-members involved in the earlier dataset are virtually unchanged except for clinochlore and, through its dependence by reactions, phlogopite (Table 7; *cf.* DS2, table A1). Some significant features of our updated and enlarged dataset are as follows:

1. The dataset is considerably larger, involving 123 mineral and fluid end-members.

2. The dataset includes Tschermak's end-members in orthopyroxene, clinopyroxene, amphibole, white mica, biotite, chlorite and talc.

3. Experimental and natural Fe:Mg partitioning has been used to incorporate Fe end-members of minerals whose magnesian counterparts had been generated from experimentally determined phase equilibria.

4. Landau theory is used to account for Al–Si order–disorder in equilibrium feldspars and other phases, as well as for end-members which have lambda heat capacity anomalies.

5. The H_2O and CO_2 contents of cordierites as a function of pressure and temperature are explicitly accounted for through the approach and expressions of Kurepin (1985).

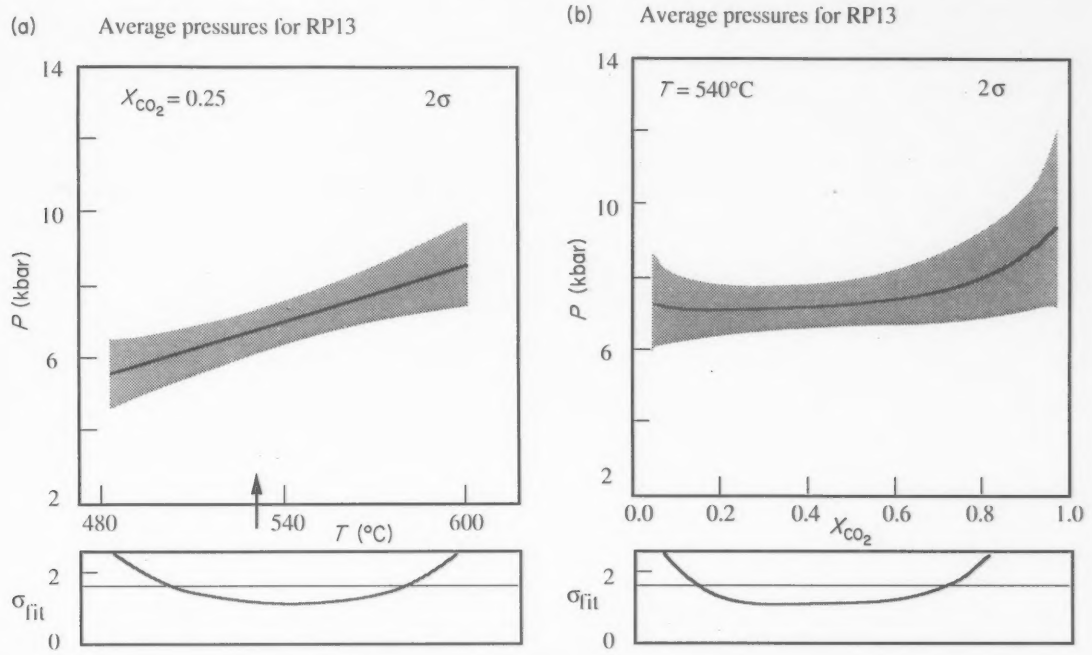

Fig. 4. Average pressures for Scottish Dalradian calc-pelite RP13; based upon ten independent reactions. Details are in Table 10. (a) Average pressures at fixed X_{CO_2} as a function of temperature, and (b) at fixed temperature as a function of X_{CO_2}.

The large number of end-members in common minerals such as micas, chlorites, amphiboles and garnets enables reliable barometry to be performed on rather 'ordinary' mineral assemblages, obviating the need to find those unusual low variance rocks in order to be able to apply more than one popular barometer. It also allows the determination of the degree to which equilibrium may or may not have been attained in natural assemblages (e.g. DS3, p. 192).

Since the publication of DS2, a new project has been completed by Berman (1988) which used linear programming techniques to generate an internally consistent dataset. The publication of the Berman dataset has significantly improved the state of knowledge for a number of minerals, and we have gained from several valuable insights made by that group. Although both datasets produce comparable results for minerals in the set of phases where there is overlap, our dataset, we believe, has the important advantage of including estimates of the uncertainties and correlations between the thermodynamic data; we consider that the necessity of estimating uncertanties in calculations, whether for rock conditions or for phase diagrams, is something which must be taken much more seriously. As shown in DS3 (p. 180), it is not at all easy to determine which equilibria will have small uncertainties and which will have large, unless the error propagations are performed.

THERMOCALC—A PROGRAM FOR PETROLOGICAL APPLICATIONS

A new, and continually evolving computer program, THERMOCALC, in IBM PC (from TJBH for £10) and Mac (from RP for A$25) versions is available from the authors, in which the calculation procedures advocated in DS3 are implemented. Use of this program allows maximum advantage to be taken of this dataset.

THERMOCALC operates in two modes, a phase diagram mode and a rock oriented mode. In phase diagram mode the user inputs the names of end-members and specifies a *P–T* window within which results are to be displayed and the program then generates all the reactions possible among the specified end-members, decides which ones lie within the window, and determines the stability level for each (stable or metastable). It also determines all intersections, and their stability levels, which occur within the window and performs a Schreinemakers analysis on each invariant point. The resulting information is tabulated along with the estimated errors for reaction and invariant point. If desired, reduced activities may be entered for any end-member—although this is not recommended (the resulting activity-corrected curves are not genuine phase diagram features).

In the rock oriented mode the program accepts a list of end-members together with associated activities (derived

typically from microprobe data) from a rock mineral assemblage and attempts to find optimum conditions of formation of that mineral assemblage. An independent set of equilibria is identified and optimum pressures at specified temperatures or optimum temperatures at specified pressures are calculated by a least squares method as described in DS3 and above for rock RP13. Thus the maximum information attainable from our dataset is used. The size of the uncertainties on calculated pressures may upset some petrologists who have become comfortable with a naïve use of conventional barometers. As noted in DS3 (p. 190) geobarometry is less precise than its practitioners would have us believe, and the problem usually lies not with the calibrations or with the thermodynamic data used for the equilibria but with poorly known activity–composition relations for the end-members in the mineral phases. THERMOCALC has a built in safety valve to guard against overoptimism in barometrists in the form of a default uncertainty applied to input activities (see discussion in DS3, p. 178 and Appendix D).

We are committed to improvement in the quality and scope of the dataset, and aim to be able to provide updated versions of the programs and data on disk at regular intervals in the future.

ACKNOWLEDGEMENTS

We wish to thank Judy Baker, Ian Buick, Michel Guiraud, David Waters and Thomas Will for their help in improving the thermodynamic data set by testing various aspects of the data in phase diagram calculations and on their own rock data. We are grateful to Greg Anderson and an anonymous reviewer for comments and criticisms, and especially thank John Brady for his perceptive, constructive and helpful review. Cambridge Earth Science Series no. 1385.

REFERENCES

Ackermand, D., Seifert, F. & Schreyer, W., 1975. Instability of sapphirine at high pressures. *Contributions to Mineralogy and Petrology*, **50**, 79–92.

Allen, J. M. & Fawcett, J. J., 1982. Zoisite–anorthite–calcite stability relations in H_2O–CO_2 fluids at 5000 bars: An experimental and SEM study. *Journal of Petrology*, **23**, 215–239.

Anovitz, L. M. & Essene, E. J., 1987. Phase equilibria in the system $CaCO_3$–$MgCO_3$–$FeCO_3$. *Journal of Petrology*, **28**, 389–414.

Anovitz, L. M., Treiman, A. H., Essene, E. J., Hemingway, B. S., Westrum, E. F. Jr., Wall, V. J., Burriel, R. & Bohlen, S. R., 1985. The heat capacity of ilmenite and phase equilibria in the system Fe–Ti–O. *Geochimica et Cosmochimica Acta*, **49**, 2027–2040.

Anderson, P. A. M., Newton, R. C. & Kleppa, O. J., 1977. The enthalpy change of the andalusite–sillimanite reaction and the Al_2SiO_5 diagram. *American Journal of Science*, **277**, 585–593.

Barnes, H. L. & Ernst, W. G., 1963. Ideality and ionization in hydrothermal fluids. The system MgO–H_2O–NaOH. *American Journal of Science*, **261**, 129–150.

Belsley, D. A., Kuh, E. & Welsch, R. E., 1980. *Regression Diagnostics*, p. 292. Wiley, New York.

Berman, R. G., 1988. Internally-consistent thermodynamic data for minerals in the system Na_2O–K_2O–CaO–MgO–FeO–Fe_2O_3–Al_2O_3–SiO_2–TiO_2–H_2O–CO_2. *Journal of Petrology*, **29**, 445–522.

Berman, R. G. & Brown, T. H., 1985. The heat capacity of minerals in the system K_2O–Na_2O–CaO–MgO–FeO–Fe_2O_3–Al_2O_3–SiO_2–TiO_2–H_2O–CO_2: representation, estimation, and high temperature extrapolation. *Contributions to Mineralogy and Petrology*, **89**, 168–183.

Berman, R. G. & Brown, T. H., 1987. Development of models for multicomponent melts: analysis of synthetic systems. In: *Reviews in Mineralogy* (eds Carmichael, I. S. E. & Eugster, H. P.) **17**, pp. 405–442. Mineralogical Society of America, Washington DC.

Birch, F., 1966. Compressibility; elastic constants In: *Handbook of Physical Constants* (ed. Clark, S. P.) *Geological Society of America Memoir*, **97**, 97–173.

Bird, G. W. & Fawcett, J. J., 1973. Stability relations of Mg-chlorite–muscovite and quartz between 5 and 10 kbar water pressure. *Journal of Petrology*, **14**, 415–428.

Boettcher, A. L., 1970. The system CaO–Al_2O_3–SiO_2–H_2O at high temperatures and pressures. *Journal of Petrology*, **11**, 337–339.

Bohlen, S. R. & Boettcher, A. L., 1982. The quartz–coesite transformation: A precise determination and the effects of other components. *Journal of Geophysical Research*, **87**, 7073–7078.

Bohlen, S. R., Boetcher, A. L., Wall, V. J. & Clements, J. D., 1983. Stability of phlogopite–quartz and sanidine–quartz: A model for melting in the lower crust. *Contributions to Mineralogy and Petrology*, **83**, 270–277.

Bohlen, S. R., Dollase, W. A. & Wall, V. J., 1986. Calibration and applications of spinel equilibria in the system FeO–Al_2O_3–SiO_2. *Journal of Petrology*, **27**, 1143–1156.

Bohlen, S. R., Essene, E. J. & Boettcher, A. L., 1980. Reinvestigation and application of olivine–quartz–orthopyroxene barometry. *Earth and Planetry Science Letters*, **47**, 1–10.

Bohlen, S. R. & Liotta, J. J., 1986. A barometer for garnet amphibolites and garnet granulites. *Journal of Petrology*, **27**, 1025–1034.

Bohlen, S. R., Metz, G. W., Essene, E. J., Anovitz, L. M., Westrum, E. F. & Wall, V. J., 1983. Thermodynamics and phase equilibrium of ferrosilite: Potential oxygen barometer in mantle rocks. *EOS* (*Transactions of the American Geophysical Union*), **64**, 350.

Bohlen, S. R., Wall, V. J. & Boettcher, A. L., 1983. Experimental investigation and application of garnet granulite equilibria. *Contributions to Mineralogy and Petrology*, **83**, 52–61.

Bohlen, S. R., Wall, V. J. & Boettcher, A. L., 1983. Experimental investigations and geological applications of equilibria in the system FeO–TiO_2–Al_2O_3–SiO_2–H_2O. *American Mineralogist*, **68**, 1049–1058.

Boyd, F. R., 1959. Hydrothermal investigations of amphiboles. In: *Researches in Geochemistry, 1* (ed. Abelson, P. H.). Wiley, New York.

Brousse, C., Newton, R. C. & Kleppa, O. J., 1984. Enthalpy of formation of forsterite, enstatite, akermanite, monticellite and merwinite at 1073 K determined by alkali borate solution calorimetry. *Geochimica et Cosmochimica Acta*, **48**, 1081–1088.

Burton, J. C., Taylor, L. A. & Chou, I.-M., 1982. The f_{O_2}–T and f_{S_2}–T stability relations of hedenbergite and of hedenbergite–johansenite solid solutions. *Economic Geology*, **77**, 764–783.

Butler, P., 1969. Mineral compositions and equilibration in the metamorphosed iron formation of the Gagnon region, Quebec, Canada. *Journal of Petrology*, **10**, 56–101.

Carman, J. H., 1974. Synthetic sodium phlogopite and its hydrates: Stabilities, properties and mineralogic implications. *American Mineralogist*, **59**, 261–273.

Carman, J. H. & Gilbert, M. C., 1983. Experimental studies on glaucophane stability. *American Journal of Science*, **283A**, 414–437.

Carpenter, M. A., 1988. Thermochemistry of aluminium/silicon ordering in feldspar minerals. In: *Physical Properties and Thermodynamic Behaviour of Minerals* (ed. Salje, E.), **C225,** pp. 265–323, NATO ASI.

Carpenter, M. A., McConnell, J. D. C. & Navrotsky, A., 1985. Enthalpies of ordering in the plagioclase feldspar solid solution. *Geochimica et Cosmochimica Acta,* **49,** 947–966.

Charlu, T. V., Newton, R. C. & Kleppa, O. J., 1975. Enthalpies of formation at 970 K of compounds in the system $MgO–Al_2O_3–SiO_2$ from high temperature solution calorimetry. *Geochimica et Cosmochimica Acta,* **39,** 487–497.

Charlu, T. V., Newton, R. C. & Kleppa, O. J., 1978. Enthalpy of formation of some lime silicates by high temperature solution calorimetry, with discussion of high pressure phase equilibria. *Geochimica et Cosmochimica Acta,* **42,** 367–375.

Charlu, T. V., Newton, R. C. & Kleppa, O. J., 1981. Thermochemistry of synthetic $Ca_2Al_2SiO_7$(gehlenite)–$Ca_2MgSi_2O_7$(akermanite) melilites. *Geochimica et Cosmochrimica Acta,* **45,** 1609–1617.

Chatillon-Colinet, C., Kleppa, O. J., Newton, R. C. & Perkins, D.III., 1983. Enthalpy of formation of $Fe_3Al_2Si_3O_{12}$ (almandine) by high temperature alkali borate solution calorimetry. *Geochimica et Cosmochimica Acta,* **47,** 439–444.

Chatterjee, N. D., 1970. Synthesis and upper stability of paragonite. *Contributions to Mineralogy and Petrology,* **27,** 244–257.

Chatterjee, N. D., 1971. The upper stability limit of the assemblage paragonite + quartz and its natural occurrences. *Contributions to Mineralogy and Petrology,* **34,** 288–303.

Chatterjee, N. D., 1974. Synthesis and upper thermal stability limit of 2M-margarite, $CaAl_2Al_2Si_2O_{10}(OH)_2$. *Schweizerische Mineralogische und Petrologische Mitteilungen,* **54,** 753–767.

Chatterjee, N. D., 1976. Margarite stability and compatibility relations in the system $CaO–Al_2O_3–SiO_2–H_2O$ as a pressure-temperature indicator. *American Mineralogist,* **61,** 699–709.

Chatterjee, N. D. & Johannes, W., 1974. Thermal stability and standard thermodynamic properties of synthetic 2M1-muscovite, $KAl_2AlSi_3O_{10}(OH)_2$. *Contributions to Mineralogy and Petrology,* **48,** 89–114.

Chatterjee, N. D., Johannes, W. & Leistner, H., 1984. The system $CaO–Al_2O_3–SiO_2–H_2O$: New phase equilibria data, some calculated phase relations, and their petrological applications. *Contributions to Mineralogy and Petrology,* **88,** 1–13.

Chernosky, J. V., 1973. The stability of chrysotile, $Mg_3Si_2O_5(OH)_4$, and the free energy of formation of talc, $Mg_3Si_4O_{10}(OH)_2$. *Geological Society of American Abstracts with Programs,* **5,** 575.

Chernosky, J. V., 1974. The upper stability of clinochlore at low pressure and the free energy of formation of Mg-cordierite. *American Mineralogist,* **59,** 496–507.

Chernosky, J. V., 1976. Gibbs free energy of enstatite, clinochlore and hydrous Mg-cordierite evaluated from phase equilibrium data. *EOS* (*Transactions of the American Geophysical Union*), **57,** 1020.

Chernosky, J. V., 1976. The stability of anthophyllite—a re-evaluation based on new experimental data. *American Mineralogist,* **61,** 1145–1155.

Chernosky, J. V., 1978. The stability of clinochlore and quartz at low pressure. *American Mineralogist,* **63,** 73–82.

Chernosky, J. V., 1982. The stability of clinochrysotile. *Canadian Mineralogist,* **20,** 19–27.

Chernosky, J. V. & Autio, L. K., 1979. The stability of anthophyllite in the presence of quartz. *American Mineralogist,* **84,** 294–300.

Chernosky, J. V. & Berman, R. G. 1986. The stability of clinochlore in mixed volatile, $CO_2–H_2O$ fluids. *EOS* (*Transactions of the American Geophysical Union*), **67,** 407.

Chernosky, J. V. & Berman, R. G., 1986. Experimental reversal of the equilibrium: Clinochlore + 2 magnesite = 3 forsterite + spinel + $2CO_2$ + $4H_2O$. *EOS* (*Transactions of the American Geophysical Union*), **67,** 1279.

Chernosky, J. V., Day, H. W. & Caruso, L. J., 1985. Equilibria in the system $MgO–SiO_2–H_2O$: experimental determination of the stability of Mg-anthophyllite. *American Mineralogist,* **70,** 223–236.

Chinner, G. A. & Dixon, J. E., 1974. Some high pressure parageneses of the Allalin Gabbro, Valais, Switzerland. *Journal of Petrology,* **14,** 185–202.

Chopin, C. & Monie, P., 1984. A unique magnesiochloritoid-bearing, high pressure assemblage from the Monte Rosa: a petrologic and 40Ar-39Ar study. *Contributions to Mineralogy and Petrology,* **87,** 388–398.

Chopin, C. & Schreyer, W., 1983. Magnesiocarpholite and magnesiochloritoid: Two index minerals of pelitic blueschists and their preliminary phase relations in the model system $MgO–Al_2O_3–SiO_2–H_2O$. *American Journal of Science,* **283A,** 72–96.

Colville, P., Ernst, W. G. & Gilbert, M. C., 1966. Relationships between cell parameters and chemical compositions of monoclinic amphiboles. *American Mineralogist,* **51,** 1727–1754.

Conolly, J. A. D. & Kerrick, D. M., 1985. Experimental and thermodynamic analysis of prehnite. *EOS* (*Transactions of the American Geophysical Union*), **66,** 388.

Crawford, W. A. & Fyfe, W. S., 1965. Lawsonite equilibria. *American Journal of Science,* **263,** 262–270.

Danckwerth, P. & Newton, R. C., 1978. Experimental determination of the spinel peridotite to garnet peridotite reaction in the system $MgO–Al_2O_3–SiO_2$ in the range 900–1100 °C and Al_2O_3 isopleths of enstatite in the spinel field. *Contributions to Mineralogy and Petrology,* **66,** 189–200.

Day, H. W. & Kumin, H. J., 1980. Thermodynamic analysis of the aluminium silicate triple point. *American Journal of Science,* **280,** 265–287.

Demarest, H. H. & Haselton, H. T. Jr., 1981. Error analysis for bracketed phase equilibrium data. *Geochimica et Cosmochimica Acta,* **45,** 217–224.

Dutrow, B. L. & Holdaway, M. J., 1986. Upper thermal stability of staurolite + quartz at medium pressures: A reinvestigation. *Terra Cognita,* **6,** 214.

Eggert, R. G. & Kerrick, D. M., 1981. Metamorphic equilibria in the siliceous dolomite system: 6 kbar experimental data and geologic implications. *Geochimica et Cosmochimica Acta,* **45,** 1039–1049.

Ernst, W. G., 1966. Synthesis and stability relations of ferrotremolite. *American Journal of Science,* **264,** 37–65.

Essene, E. J., Wall, V. J. & Westrum, E. F., 1980. Thermodynamic properties and phase equilibria for fayalite. *Geological Society of American Abstracts with Programs,* **12,** 422.

Fawcett, J. J. & Yoder, H. S., 1966. Phase relationships of chlorites in the system $MgO–Al_2O_3–SiO_2–H_2O$. *American Mineralogist,* **61,** 303–310.

Ferry, J. M. & Spear, F. S., 1978. Experimental calibration of the partitioning of Fe and Mg between biotite and garnet. *Contributions to Mineralogy and Petrology,* **66,** 113–117.

Finger, L. W. & Hazen, R. M., 1980. Crystal structure and isothermal compression of Fe_2O_3, Cr_2O_3, and V_2O_3 to 50 kbars. *Journal of Applied Physics,* **51,** 5362–5367.

Finger, L. W., Hazen, R. M. & Hofmeister, A., 1986. High pressure crystal chemistry of spinel ($MgAl_2O_4$) and magnetite (Fe_3O_4): comparisons with other silicate spinels. *Physics and Chemistry of Minerals,* **13,** 215–220.

Fonarev, V. I. & Konilov, A. N., 1986. Experimental study of Fe-Mg distribution between biotite and orthopyroxene. *Contributions to Mineralogy and Petrology,* **93,** 227–235.

Fonarev, V. I. & Korolkov, G. J., 1980. The assemblage orthopyroxene + cummingtonite + quartz. The low-temperature stability limit. *Contributions to Mineralogy and Petrology,* **73,** 413–420.

French, B. M., 1971. Stability relations of siderite ($FeCO_3$) in the system Fe–C–O. *American Journal of Science,* **271,** 37–78.

Ganguly, J., 1969. Chloritoid stability and related paragenesis:

Theory, experiments and applications. *American Journal of Science*, **267**, 910–944.

Ganguly, J., 1972. Staurolite and related paragenesis: Theory, experiments and applications. *Journal of Petrology*, **13**, 335–365.

Ganguly, J. & Newton, R. C., 1968. Thermal stability of chloritoid at high pressures and relatively high oxygen fugacities. *Journal of Petrology* **9**, 444–466.

Gasparik, T., 1984. Experimental study of subsolidus phase relations and mixing properties of pyroxene in the system CaO–Al_2O_3–SiO_2. *Geochimica et Cosmochimica Acta*, **48**, 2537–2545.

Gasparik, T., 1985. Experimental study of subsolidus phase relations and mixing properties of pyroxene and plagioclase in the system Na_2O–CaO–Al_2O_3–SiO_2. *Contributions to Mineralogy and Petrology*, **89**, 346–357.

Gasparik, T. & Newton, R. C., 1984. The reversed alumina contents of orthopyroxene in equilibrium with spinel and forsterite in the system MgO–Al_2O_3–SiO_2. *Contributions to Mineralogy and Petrology*, **85**, 186–196.

Goldsmith, J. R., 1980. The melting and breakdown reactions of anorthite at high pressures and temperatures. *American Mineralogist*, **65**, 272–284.

Goldsmith, J. R., 1981. The join $CaAl_2Si_2O_8$–H_2O (anorthite–water) at elevated pressures and temperatures. *American Mineralogist*, **66**, 1183–1188.

Goldsmith, J. R., 1980. Thermal stability of dolomite at high temperatures and pressures. *Journal of Geophysical Research*, **85**, 6949–6954.

Goldsmith, J. R. & Heard, H. C., 1962. Subsolidus phase relations in the system $CaCO_3$–$MgCO_3$. *Journal of Geology*, **69**, 45–74.

Goldsmith, J. R. & Newton, R. C., 1977. Scapolite–plagioclase stability relations at high pressures and temperatures in the system $NaAlSi_3O_8$–$CaAl_2Si_2O_8$–$CaCO_3$–$CaSO_4$. *American Mineralogist*, **62**, 1063–1081.

Goldsmith, J. R., Witters, J. & Northrup, D. A., 1962. Studies in the system $CaCO_3$–$MgCO_3$–$FeCO_3$: a method for major element spectrochemical analysis; 3. Composition of some ferroan dolomites. *Journal of Geology*, **70**, 659–687.

Gordon, T. M. & Greenwood, H. J., 1970. The reaction: dolomite + quartz + water = talc + calcite + carbon dioxide. *American Journal of Science*, **268**, 225–242.

Green, T. H. & Hellman, P. L., 1982. Fe-Mg partitioning between coexisting garnet and phengite at high pressure, and comments on a garnet-phengite geothermometer. *Lithos*, **15**, 253–266.

Greenwood, H. J., 1967. Wollastonite: Stability in H_2O–CO_2 mixtures and occurrence in a contact-metamorphic aureole near Salmo, British Columbia, Canada. *American Mineralogist*, **52**, 1669–1680.

Greenwood, H. J., 1967. Mineral equilibria in the system MgO–SiO_2–H_2O–CO_2. In: *Researches in Geochemistry II* (ed. Abelson, P. H.), pp. 542–547, Wiley, New York.

Gronvold, F. & Sveen, A., 1974. Heat capacity and thermodynamic properties of synthetic magnetite (Fe_3O_4) from 300 to 1050 K. Ferrimagnetic transition and zero-point entropy. *Journal of Chemical Thermodynamics*, **6**, 859–872.

Guiraud, M., Holland, T. J. B. & Powell, R., 1989. Calculated mineral equilibria in the greenschist–blueschist–eclogite facies in Na_2O–FeO–MgO–Al_2O_3–SiO_2–H_2O. *Contributions to Mineralogy and Petrology*, in press.

Haas, H., 1972. Diaspore-corundum equilibrium determined by epitaxis of diaspore on corundum. *American Mineralogist*, **57**, 1375–1385.

Haas, H. & Holdaway, M. J., 1973. Equilibria in the system Al_2O_3–SiO_2–H_2O involving the stability limits of pyrophyllite and the thermodynamic data of pyrophyllite. *American Journal of Science*, **273**, 449–464.

Harker, R. I., 1959. The synthesis and stability of tilleyite, $Ca_5Si_2O_7(CO_3)_2$. *American Journal of Science*, **257**, 656–667.

Harker, R. I. & Tuttle, O. F., 1955. Studies in the system CaO–MgO–CO_2. Part 1: the thermal dissociation of calcite, dolomite and magnesite. *American Journal of Science*, **253**, 209–224.

Harker, R. I. & Tuttle, O. F., 1956. Experimental data on the P_{CO_2}–T curve for the reaction: calcite + quartz = wollastonite + carbon dioxide. *American Journal of Science*, **254**, 239–256.

Harker, R. I. & Tuttle, O. F., 1956. The lower stability limit of akermanite ($Ca_2MgSi_2O_7$). *American Journal of Science*, **254**, 468–478.

Harley, S. L., 1984. An experimental study of the partitioning of Fe and Mg between garnet and orthopyroxene. *Contributions to Mineralogy and Petrology*, **86**, 359–373.

Harte, B. & Hudson, N. F. C., 1979. Pelite facies series and the temperatures and pressures of Dalradian metamorphism in eastern Scotland. In: *The Caledonides of the British Isles Reviewed* (eds Harris, A. L., Holland, C. H. & Leake, B. E.), Geological Society of London Special Publications, 8, 323–337.

Haselton, H. T., Jr., Hemingway, B. S. & Robie, R. A., 1982. Low temperature heat-capacity measurements on synthetic $CaAl_2SiO_6$ pyroxene. *EOS* (*Transactions of the American Geophysical Union*), **63**, 467.

Haselton, H. T. Jr., Hemingway, B. S. & Robie, R. A., 1984. Low temperature heat capacities of $CaAl_2SiO_6$ glass and pyroxene and thermal expansion of $CaAl_2SiO_6$ pyroxene. *American Mineralogist*, **69**, 481–489.

Haselton, H. T. Jr., Robie, R. A. & Hemingway, B. S., 1987. Heat capacities of synthetic hedenbergite, ferrobustamite and $CaFeSi_2O_6$ glass. *Geochimica et Cosmochimica Acta*, **51**, 2211–2217.

Haselton, H. T. Jr., Sharp, W. R. & Newton, R. C., 1978. CO_2 fugacity at high temperatures and pressures from experimental decarbonation reactions. *Geophysical Research Letters*, **5**, 753–756.

Hays, J. F., 1967. Lime-alumina-silica. *Carnegie Institute of Washington Yearbook*, **65**, 234–239.

Hazen, R. M. 1977. Effects of temperature and pressure on the crystal structure of ferromagnesian olivine. *American Mineralogist*, **62**, 286–295.

Hazen, R. M., & Finger, L. W. 1978. The crystal structures and compressibilities of layer minerals at high pressure. II. Phlogopite and chlorite. *American Mineralogist*, **63**, 293–296.

Heinrich, W. & Althaus, E., 1980. Die obere Stabilitätsgrenze von Lawsonit plus Albit bzw Jadeit. *Fortschritte der Mineralogie*, **58**, 49–50.

Helgeson, H. C., Delany, J. M., Nesbitt, H. W. & Bird, D. K., 1978. Summary and critique of the thermodynamic properties of rock-forming minerals. *American Journal of Science*, **278A**, 229 pp.

Hemingway, B. S., 1987. Quartz: Heat capacities from 340 to 1000 K and revised values for the thermodynamic properties. *American Mineralogist*, **72**, 273–279.

Hemingway, B. S., Evans, H. T., Nord, G. L., Haselton, H. T., Robie, R. A. & McGee, J. J., 1986. Akermanite: Phase transitions in heat capacity and thermal expansion, and revised thermodynamic data. *Canadian Mineralogist*, **24**, 425–434.

Hemingway, B. S. & Robie, R. A., 1984. Heat capacity and thermodynamic functions for gehlenite and staurolite: with comments on the Schottky anomaly in the heat capacity of staurolite. *American Mineralogist*, **69**, 307–318.

Henderson, C. E., Essene, E. J., Anovitz, L. M., Westrum, E. F., Hemingway, B. S. & Bowman, J. R., 1983. Thermodynamics and phase equilibria of clinochlore $(Mg_5Al)(Si_3Al)_{10}(OH)_8$. *EOS* (*Transactions of the American Geophysical Union*), **64**, 466.

Hertzberg, C. T., 1983. The reaction forsterite + cordierite = aluminous orthopyroxene + spinel in the system MgO–Al_2O_3–SiO_2. *Contributions to Mineralogy and Petrology*, **84**, 84–90.

Hewitt, D. A., 1973. Stability of the assemblage muscovite–calcite–quartz. *American Mineralogist*, **58**, 785–791.

Hewitt, D. A., 1975. Stability of the assemblage phlogopite–calcite–quartz. *American Mineralogist*, **60**, 391–397.

Hewitt, D. A. & Wones, D. R., 1975. Physical properties of some

synthetic Fe–Mg–Al trioctahedral biotites. *American Mineralogist*, **60**, 854–862.

Hochella, M. F., Liou, J. G., Keskinen, M. J. & Kim, H. S., 1982. Synthesis and stability relations of magnesian idocrase. *Economic Geology*, **77**, 798–808.

Hoffmann, C., 1972. Natural and synthetic ferroglaucophane. *Contributions to Mineralogy and Petrology*, **34**, 135–149.

Holdaway, M. J., 1971. Stability of andalusite and the aluminum silicate phase diagram. *American Journal of Science*, **271**, 97–131.

Holdaway, M. J.,Dutrow, B. L., Borthwick, J., Shore, P., Harmon, R. S. & Hinton, R. W., 1987. H content of staurolite as determined by H extraction line and ion microprobe. *American Mineralogist*, **71**, 1135–1142.

Holdaway, M. J. & Lee, S. M., 1977. Fe–Mg cordierite stability in high-grade pelitic rocks based on experimental, theoretical and natural observations. *Contributions to Mineralogy and Petrology*, **63**, 175–198.

Holland, T. J. B., 1979. Experimental determination of the reaction paragonite = jadeite + kyanite + quartz + water, and internally consistent thermodynamic data for part of the system Na_2O–Al_2O_3–SiO_2–H_2O, with applications to eclogites and blueschists. *Contributions to Mineralogy and Petrology*, **68**, 293–301.

Holland, T. J. B., 1980. The reaction albite = jadeite + quartz determined experimentally in the range 600–1200 °C. *American Mineralogist*, **65**, 129–134.

Holland, T. J. B., 1984. Stability relations of ortho- and clinozoisite. *NERC Progress in Experimental Petrology, Progress Report* **6**, 185–186.

Holland, T. J. B., 1988. Preliminary phase relations involving glaucophane and applications to high pressure petrology: heat capacity and thermodynamic data. *Contributions to Mineralogy and Petrology*, **99**, 134–142.

Holland, T. J. B. 1989. the dependence of entropy on volume for silicate and oxide minerals: a review and a predictive model. *American Mineralogist*, **74**, 5–13.

Holland, T. J. B., Navrotsky, A. & Newton, R. C., 1979. Thermodynamic parameters of $CaMgSi_2O_6$–$Mg_2Si_2O_6$ pyroxenes based on regular solution and cooperative disordering models. *Contributions to Mineralogy and Petrology*, **69**, 337–344.

Holland, T. J. B. & Powell, R., 1985. An internally consistent thermodynamic dataset with uncertainties and correlations: 2. Data and results. *Journal of Metamorphic Geology*, **3**, 343–370.

Holm, J. L. & Kleppa, O. J., 1966. The thermodynamic properties of the aluminum silicates. *American Mineralogist*, **51**, 1608–1622.

Hoschek, G., 1973. Die Reaktion Phlogopit + Calcit + Quartz = Tremolit + Kalifeldspat + H_2O + CO_2. *Contributions to Mineralogy and Petrology*, **39**, 231–237.

Hoschek, G., 1974. Gehlenite stability in the system CaO–Al_2O_3–SiO_2–H_2O–CO_2. *Contributions to Mineralogy and Petrology*, **47**, 245–254.

Hsu, L. C., 1968. Selected phase relationships in the system Al–Mn–Fe–Si–O; a model for garnet equilibria. *Journal of Petrology*, **9**, 40–83.

Huang, W. L. & Wyllie, P. J., 1975. Melting and subsolidus phase relationships for $CaSiO_3$ to 35 kilobars pressure. *American Mineralogist*, **60**, 213–217.

Huckenholz, H. G., Holzl, E., & Lindhuber, W., 1975. Grossularite, its solidus and liquidus relations in the system CaO–Al_2O_3–SiO_2–H_2O up to 10 kbars. *Neues Jahrbuch für Mineralogie Abhandlungen*, **124**, 1–46.

Huckenholz, H. G. & Yoder, H. S., 1971. Andradite stability relations in the $CaSiO_3$–Fe_2O_3 join up to 30 kb. *Neues Jahrbuch für Mineralogie Abhandlungen*, **114**, 246–280.

Huebner, J. S., 1969. Stability relations of rhodachrosite in the system manganese–carbon–oxygen. *American Mineralogist*, **54**, 457–481.

Huebner, J. S., & Eugster, H. P., 1968. Rhodachrosite decarbonation in the system MnO–SiO_2–CO_2. *Geological Society of America Special Publication*, **121**, 144–145.

Hunt, J. A., & Kerrick, D. M., 1977. The stability of sphene: experimental redetermination and geological implications. *Geochimica et Cosmochimica Acta*, **41**, 279–288.

Irving, A. J., Huang, W. L. & Wyllie, P. J., 1977. Phase relations of portlandite, $Ca(OH)_2$ and brucite, $Mg(OH)_2$ to 33 kilobars. *American Journal of Science*, **277**, 313–321.

Irving, A. J. & Wyllie, P. J., 1975. Subsolidus and melting relationships for calcite, magnesite, and the join $CaCO_3$–$MgCO_3$ to 36 kb. *Geochimica et Cosmochimica Acta*, **39**, 35–53.

Ivaldi, G., Catti, M. & Ferraris, G., 1988. Crystal structure at 25 and 700° of magnesiochloritoid from a high pressure assemblage (Monte Rosa). *American Mineralogist*, **73**, 358–364.

Jacobs, G. K. & Kerrick, D. M., 1979. Experimental and thermodynamic analysis of decarbonation reactions and the high temperature heat capacity of calcite. *EOS* (*Transactions of the American Geophysical Union*), **60**:**18**, 406.

Jacobs, G. K. & Kerrick, D. M., 1981. Devolatilization equilibria in H_2O–CO_2 and H_2O–CO_2–NaCl fluids: an experimental and thermodynamic evaluation at elevated pressures and temperatures. *American Mineralogist*, **66**, 1135–1153.

Jenkins, D. M., 1981. Experimental phase relations of hydrous peridotites modelled in the system H_2O–CaO–MgO–SiO_2. *Contributions to Mineralogy and Petrology*, **77**, 166–176.

Jenkins, D. M., 1983. Stability and composition relations of calcic amphiboles in ultramafic rocks. *Contributions to Mineralogy and Petrology*, **83**, 375–384.

Jenkins, D. M., 1984. Upper pressure stability of synthetic margarite + quartz. *Contributions to Mineralogy and Petrology*, **88**, 332–339.

Jenkins, D. M. & Chernosky, J. V. Jr., 1986. Phase equilibria and crystallochemical properties of Mg-chlorite. *American Mineralogist*, **71**, 924–936.

Jenkins, D. M., Newton, R. C., & Goldsmith, J. G., 1983. Fe-free clinozoisite stability relative to zoisite. *Nature*, **304**, 622–623.

Johannes, W., 1968. Experimental investigation of the reaction forsterite + H_2O = serpentine + brucite. *Contributions to Mineralogy and Petrology*, **19**, 309–315.

Johannes, W., 1969. An experimental investigation of the system MgO–SiO_2–H_2O–CO_2. *American Journal of Science*, **267**, 1083–1104.

Johannes, W., 1980. Melting and subsolidus reactions in the system K_2O–CaO–Al_2O_3–SiO_2–H_2O. *Contributions to Mineralogy and Petrology*, **74**, 29–34.

Johannes, W., 1984. Beginning of melting in the granite system Qz–Or–Ab–An–H_2O. *Contributions to Mineralogy and Petrology*, **86**, 264–273.

Johannes, W. & Puhan, D., 1971. The calcite–aragonite transition re-investigated. *Contributions to Mineralogy and Petrology*, **31**, 28–38.

Käse, H.-R. & Metz, P., 1980. Experimental investigation of the metamorphism of siliceous dolomites. *Contributions to Mineralogy and Petrology*, **73**, 151–159.

Kawasaki, T. & Matsui, Y., 1983. Thermodynamic analysis of equilibria involving olivine, orthopyroxene and garnet. *Geochimica et Cosmochimica Acta*, **47**, 1661–1680.

Kennedy, C. S., & Kennedy, G. C., 1976. The equilibrium boundary between graphite and diamond. *Journal of Geophysical Research*, **81**, 2467–2470.

Kerrick, D. M., 1968. Experiments on the upper stability limits of pyrophyllite at 1.8 kbar and 3.9 kbar water pressure. *American Journal of Science*, **266**, 204–214.

Kerrick, D. M. & Heninger, G. S., 1984. The andalusite–sillimanite equilibrium revisited. *Geological Society of America Abstracts with Programs*, **16**, 558.

Kitahara, S., Takenouchi, S. & Kennedy, G. C., 1966. Phase relations in the system MgO–SiO_2–H_2O at high temperatures and pressures. *American Journal of Science*, **264**, 223–233.

Klein, C., 1978. Regional metamorphism of Proterozoic

iron-formation, Labrador Trough, Canada. *American Mineralogist*, **63**, 898–912.

Ko, H. C., Ferrante, M. J. & Stuve, J. M., 1977. Thermophysical properties of acmite. In: *Proceedings of the 7th Symposium on Thermophysical Properties. Washington D.C.* (*American Society of Mechanical Engineers*), pp. 392–395.

Koziol, A. & Newton, R. C., 1986. Definition of anorthite = grossular + kyanite + quartz in the range 650–1250 °C. *Geological Society of America Abstracts with Programs*, **188**, 661.

Krogh, E. J. & Råheim, A., 1978. Temperature and pressure dependence of Fe–Mg partitioning between garnet and phengite, with particular reference to eclogites. *Contributions to Mineralogy and Petrology*, **66**, 75–80.

Kulke, H., & Schreyer, W., 1973. Kyanite–talc schist from Sar e Sang, Afghanistan. *Earth and Planetary Science Letters*, **18**, 324–328.

Kurepin, V. A., 1985. H_2O and CO_2 contents of cordierite as an indicator of thermodynamic conditions of formation. *Geochemistry International*, **22**, 148–156.

Lager, G. A. & Meagher, E. P. 1978. High-temperature study of six olivines. *American Mineralogist*, **63**, 365–377.

Lange, R. A., Carmichael, I. S. E. & Stebbins, J. F., 1986. Phase transitions in leucite $KAlSiO_6$, orthorhombic $KAlSiO_4$, and their iron analogues ($KFeSi_2O_6$, $KFeSiO_4$). *American Mineralogist*, **71**, 937–945.

Latard, D. & Schreyer, W., 1981. Experimental results bearing on the stability of the blueschist facies minerals deerite, howieite, and zussmanite, and their petrological significance. *Bulletin Mineralogique*, **104**, 431–440.

Lee, H. Y. & Ganguly, J., 1988. Equilibrium compositions of coexisting garnet and orthopyroxene: experimental determinations in the system $FeO–MgO–Al_2O_3–SiO_2$, and applications. *Journal of Petrology*, **29**, 93–113.

Levien, L. & Prewitt, C. T., 1981. High pressure crystal structure and compressibility of coesite. *American Mineralogist*, **66**, 324–333.

Lindsley, D. H., 1966. *P–T* projection for part of the system kalsilite–silica. *Carnegie Institute of Washington Yearbook*, **65**, 244–247.

Lindsley, D. H., 1981. The formation of pigeonite on the join hedenbergite-ferrosilate at 11.5 kbar: experiments and a solution model. *American Mineralogist*, **66**, 1175–1182.

Lindsley, D. H., 1983. Pyroxene thermometry. *American Mineralogist*, **68**, 477–493.

Liou, J. G., 1971. Synthesis and stability of prehnite, $Ca_2Al_2Si_3O_{10}(OH)_2$. *American Mineralogist*, **56**, 507–531.

Liou, J. G., 1973. Synthesis and stability relations of epidote, $Ca_2Al_2FeSi_3O_{12}(OH)$. *Journal of Petrology*, **14**, 381–413.

Liou, J. G., 1974. Stability relations of andradite–quartz in the system Ca–Fe–Si–O–H. *American Mineralogist*, **59**, 1016–1025.

Luth, W. C., 1967. Studies in the system $KAlSiO_4–Mg_2SiO_4–SiO_2–H_2O$: Inferred phase relations and petrologic applications. *Journal of Petrology*, **8**, 372–416.

Maresch, W. W. & Mottana, A., 1976. The pyroxmangite–rhodonite transformation for the $MnSiO_3$ composition. *Contributions to Mineralogy and Petrology*, **55**, 69–70.

Massone, H.-J., 1989. The upper thermal stability of chlorite + quartz: an experimental study in the system $MgO–Al_2O_3–SiO_2–H_2O$. *Journal of Metamorphic Geology*, **7**, 567–582.

Massonne, H.-J. & Schreyer, W., 1986. High pressure syntheses and X-ray properties of white micas in the system $K_2O–MgO–Al_2O_3–SiO_2–H_2O$. *Neues Jahrbuch für Mineralogie Abhandlungen*, **153**, 177–215.

Massonne, H.-J. & Schreyer, W., 1987. Phengite geobarometry based on the limiting assemblage with K-feldspar, phlogopite, and quartz. *Contributions to Mineralogy and Petrology*, **96**, 212–224.

Massonne, H. J., Mirwald, P. W. & Schreyer, W., 1981. Experimentelle der Reaktionskurve Chlorit + Quartz = Talk + Disthen im System $MgO–Al_2O_3–SiO_2–H_2O$. *Fortschritte der Mineralogie*, **59**, 122–123.

Matsui, Y. & Nishizawa, O., 1974. Iron (II)-magnesium exchange equilibrium between olivine and calcium-free pyroxene over a temperature range 800 to 1300°. *Bulletin de Societe de Mineralogie et de Cristallographie*, **97**, 122–130.

Matsushima, S., Kennedy, G. C., Akella, J. & Haygarth, J., 1967. A study of the equilibrium relations in the systems $Al_2O_3–SiO_2–H_2O$ and $Al_2O_3–H_2O$. *American Journal of Science*, **265**, 28–44.

Metz, P., 1976. Experimental investigation of the metamorphism of siliceous dolomites III. Equilibrium data for the reaction tremolite + 11 dolomite = 8 forsterite + 13 calcite + $9CO_2$ + H_2O. *Contributions to Mineralogy and Petrology*, **58**, 137–148.

Metz, P. & Puhan, D., 1971. Korrektur zur arbeit 'Experimentelle untersuchung der metamorphose von kieselig dolomitischen sedimenten 1. Die gleichgewichtsdaten der reaktion 3 dolomit + quartz + H_2O = talc + 3 calcite + $3CO_2$'. *Contributions to Mineralogy and Petrology*, **31**, 169–170.

Metz, G. W., Anovitz, L. M., Essene, E. J., Bohlen, S. R., Westrum, E. F. & Wall, V. J., 1983. The heat capacity and phase equilibria of almandine. *EOS* (*Transactions of the American Geophysical Union*), **64**, 346.

Miller, Ch., 1986. Alpine high-pressure metamorphism in the Eastern Alps. *Schweitzerische Mineralogische und Petrologische Mitteilungen*, **66**, 139–144.

Mirwald, P. W. & Massonne, H.-J., 1980. The low-high quartz and quartz–coesite transition to 40 kbar between 600 and 1600 °C and some reconnaissance data on the effect of the $NaAlO_2$ component on the quartz–coesite transition. *Journal of Geophysical Research*, **85**, 6983–6990.

Miyano, T. & Klein, C., 1986. Fluid behaviour and phase relations in the system Fe–Mg–Si–C–O–H. Application to high grade metamorphism of iron formations. *American Journal of Science*, **286**, 540–575.

Moecher, D. P., Essene, E. J. and Westrum, E. F., 1985. S_{298} of an intermediate scapolite and phase equilibrium constraints on Al–Si disorder. *EOS* (*Transactions of the American Geophysical Union*), **66**, 390.

Moore, P. B. & Araki, T., 1972. Atomic arrangement of merwinite, $Ca_3Mg[SiO_4]_2$, an unusual dense-packed structure of geophysical interest. *American Mineralogist*, **57**, 1355–1374.

Myers, J. & Eugster, H. P., 1983. The system Fe–Si–O: Oxygen buffer calibration to 1500 K. *Contributions to Mineralogy and Petrology*, **82**, 75–90.

Newton, R. C., 1965. The thermal stability of zoisite. *Journal of Geology*, **73**, 431–441.

Newton, R. C., 1966a. Kyanite–sillimanite equilibrium at 750 °C. *Science*, **151**, 1222–1225.

Newton, R. C., 1966c. Some calcite–silicate equilibrium relations. *American Journal of Science*, **264**, 204–222.

Newton, R. C., 1972. An experimental determination of the high pressure stability limits of magnesian cordierite under wet and dry conditions. *Journal of Geology*, **80**, 398–420.

Newton, R. C. & Kennedy, G. C., 1963. Some equilibrium relations on the join $CaAl_2Si_2O_6–H_2O$. *Journal of Geophysical Research*, **68**, 2967–2983.

Newton, R. C. & Smith, J. V. 1967. Investigation concerning the breakdown of albite at depth in the earth. *Journal of Geology*, **75**, 268–286.

Newton, R. C. & Wood, B. J. 1978. Volume behaviour of silicate solid solutions. *American Mineralogist*, **65**, 733–745.

Newton, R. C. & Wood, B. J., 1979. Thermodynamics of water in cordierite and some petrologic consequences of cordierite as a hydrous phase. *Contributions to Mineralogy and Petrology*, **68**, 391–405.

Nishiyama, T., Uehara, S. & Shinno, I., 1986. Chromian omphacite from low-grade metamorphic rocks, Nishisonogi, Kyushu, Japan. *Journal of Metamorphic Geology*, **4**, 69–77.

Nitsch, K.-H., 1972. Das $P–T–X_{CO_2}$-Stabilitätsfeld von Lawsonit. *Contributions to Mineralogy and Petrology*, **34**, 116–134.

Nitsch, K.-H., 1974. Neue Erkentnisse zur Stabilitat fur Lawsonit. *Fortschritte der Mineralogie*, **51**, 34–35.

Nitsch, K.-H., Storre, B. & Topfer, U., 1981. Experimentelle bestimmung der gleichgewichtsdaten die reaktion Margarit + Quartz = Anorthit + Andalusit/Disthen + H_2O. *Fortschritte der Mineralogie*, **59**, 139–140.

O'Neill, H. St. C. & Wood, B. J., 1979. An experimental study of Fe–Mg partitioning between garnet and olivine and its calibration as a geothermometer. *Contributions to Mineralogy and Petrology*, **70**, 59–70.

Osborn, E. F., & Shairer, J. F., 1941. The ternary system pseudowollastonite-akermanite-gehlenite. *American Journal of Science*, **239**, 713–763.

Perkins, D., III, The stability of Mg-rich garnet in the system $CaO–MgO–Al_2O_3–SiO_2$ at 1000–1300 °C and high pressure. *American Mineralogist*, **68**, 355–364.

Perkins, D., III., Essene, E. J., Westrum, E. F. & Wall, V. J., 1977. Application of new thermodynamic data to grossular phase relations. *Contributions to Mineralogy and Petrology* **64**, 137–147.

Perkins, D., III., Holland, T. J. B. & Newton, R. C., 1981. The Al_2O_3 contents of enstatite in equilibrium with garnet in the system $MgO–Al_2O_3–SiO_2$ at 15–40 kbar and 900–1600 °C. *Contributions to Mineralogy and Petrology*, **78**, 99–109.

Perkins, D. III., Westrum, E. F. & Essene, E. J., 1980. The thermodynamic properties and phase relations of some minerals in the system $CaO–Al_2O_3–SiO_2–H_2O$. *Geochimica et Cosmochimica Acta*, **44**, 61–84.

Peters, T., 1971. Pyroxmangite: stability in $H_2O–CO_2$ mixtures at a total pressure of 2000 bars. *Contributions to Mineralogy and Petrology*, **32**, 267–273.

Powell, R., 1985. Geothermometry and geobarometry: a discussion. *Journal of the Geological Society, London*, **142**, 29–38.

Powell, R. & Holland, T. J. B., 1985. An internally consistent thermodynamic dataset with uncertainties and correlations: 1. Methods and a worked example. *Journal of Metamorphic Geology*, **3**, 327–342.

Powell, R., & Holland, T. J. B., 1988. An internally consistent thermodynamic dataset with uncertainties and correlations: 3. Applications to geobarometry, worked examples and a computer program. *Journal of Metamorphic Geology*, **6**, 173–204.

Powell, R., & Holland, T. J. B., 1989. Calculated mineral equilibria in the pelite system. KFMASH ($K_2O–FeO–MgO–Al_2O_3–SiO_2–H_2O$). *American Mineralogist*, in press.

Puhan, D., 1978. Experimental study of the reaction: dolomite + K-feldspar + H_2O = phlogopite + calcite + CO_2 at the total gas pressure of 4000 and 6000 bars. *Neues Jahrbuch für Mineralogie Monatschefte*, **3**, 110–127.

Puhan, D., & Johannes, W., 1974. Experimentelle untersuchung der reaktion Dolomit + Kalifeldspat + H_2O = phlogopit + calcit + CO_2. *Contributions to Mineralogy and Petrology*, **48**, 23–31.

Rao, B., & Johannes, W., 1979. Further data on the stability of staurolite + quartz. *Neues Jahrbuch für Mineralogie Monatshefte*, 437–447.

Rice, J. M., 1977. Progressive metamorphism of impure dolomitic limestone in the Marysville aureole, Montana. *American Journal of Science*, **277**, 1–24.

Richardson, S. W., 1968. Staurolite stability in a part of the system Fe–Al–Si–O–H. *Journal of Petrology*, **9**, 467–488.

Richardson, S. W., Bell, P. M., & Gilbert, M. C., 1968. Kyanite–sillimanite equilibrium between 700 and 1500 °C. *American Journal of Science*, **266**, 513–541.

Richardson, S. W., Gilbert, M. C. & Bell, P. M., 1969. Experimental determination of kyanite–andalusite and andalusite–sillimanite equilibria; the aluminium silicate triple point. *American Journal of Science*, **267**, 259–272.

Robertson, E. C., Birch, A. F. & MacDonald, G. J. F., 1957. Experimental determination of jadeite stability relations between 700 and 1500 °C. *American Journal of Science*, **255**, 115–137.

Robie, R. A., Bethke, P. E. & Beardsley, K. M., 1967. Selected X-ray crystallographic data, molar volumes, and densities of minerals and related substances. *United States Geological Survey Bulletin*, **1248**, 87 pp.

Robie, R. A., Finch, C. B. & Hemingway, B. S., 1982. Heat capacity and entropy of fayalite (Fe_2SiO_4) between 5.1 and 383 K: Comparison of calorimetric and equilibrium values for the QFM buffer reaction. *American Mineralogist*, **67**, 463–469.

Robie, R. A., Haselton, H. T. Jr. & Hemingway, B. S., 1984. Heat capacities and entropies of rhodachrosite ($MnCO_3$) and siderite ($FeCO_3$) between 5 and 600 K. *American Mineralogist*, **69**, 349–357.

Robie, R. A., & Hemingway, B. S., 1984. Heat capacities and entropies of phlogopite ($KMg_3\{AlSi_3O_{10}\}(OH)_2$ and paragonite ($NaAl_2\{AlSi_3O_{10}\}(OH)_2$) between 5 and 900 K and estimates of the enthalpies and Gibbs free energies of formation. *American Mineralogist*, **69**, 858–868.

Robie, R. A., Hemingway, B. S. & Fisher, J. R., 1979. Thermodynamic properties of minerals and related substances at 298.15 K and 1 bar (10^5 Pascals) pressure and at higher temperatures. *United States Geological Survey Bulletin*, **1452**, 456 pp.

Robie, R. A., Hemingway, B. S. & Takei, H., 1982b. Heat capacities and entropies of Mg_2SiO_4, Mn_2SiO_4, and Ca_2SiO_4 between 5 and 380 K. *American Mineralogist*, **67**, 470–482.

Robie, R. A., Zhao, B., Hemingway, B. S. & Barton, M. S., 1987. Heat capacity and thermodynamic properties of andradite garnet, $Ca_3Fe_2Si_3O_{12}$, between 10 and 1000 K and revised values for $\Delta_f G'm$ (298, 15 K) of hedenbergite and wollastonite. *Geochimica et Cosmochimica Acta*, **51**, 2219–2224.

Robinson, P., Spear, F. S., Schumacher, J. C., Laird, J., Klein, C., Evans, B. W. & Doolan, B. L., 1982. Phase relations of metamorphic ampbiboles: natural occurrences and theory. In: *Reviews in mineralogy, vol 9B, Amphiboles: petrology and experimental phase relations*, (eds Veblen, D. & Ribbe, P.).

Rosenberg, P. E., 1967. Subsolidus relations in the system $CaCO_3–MgCO_3–FeCO_3$ between 350 and 550 °C. *American Mineralogist*, **52**, 787–797.

Salje, E., Kuscholke, B., Wruck, B. & Kroll, H., 1985. Thermodynamics of sodium feldspar II: experimental results and numerical calculations. *Physics and Chemistry of Minerals*, **12**, 99–107.

Sandrone, R., Learsi, L., Rossetti, P. & Compagnoni, R., 1986. *P–T* conditions for the eclogitic re-equilibration of the metaophiolites from the Val d'Ala di Lanzo (internal Piemontese zone, Western Alps). *Journal of Metamorphic Geology*, **4**, 161–178.

Scarfe, C. M., Luth, W. C. & Tuttle, O. F., 1966. An experimental study bearing on the absence of leucite in plutonic rocks. *American Mineralogist*, **51**, 726–735.

Schiffman, P. & Liou, J. G., 1980. Synthesis and stability relations of Mg–Al pumpellyite, $Ca_4Al_5MgSiO_{21}(OH)_7$. *Journal of Petrology*, **21**, 441.

Schramke, J. A., Kerrick, D. M. & Blencoe, J. G., 1982. The experimental determination of the brucite = periclase + H_2O equilibrium with a new volumetric technique. *American Mineralogist*, **67**, 269–276.

Schreyer, W., 1968. A reconnaissance study of the system $MgO–Al_2O_3–SiO_2–H_2O$ at pressures between 10 and 25 kb. *Carnegie Institute of Washington Yearbook*, **66**, 380–392.

Schreyer, W. & Seifert, f., 1969. High pressure phases in the system $MgO–Al_2O_3–SiO_2–H_2O$. *American Journal of Science*, **267A**, 407–443.

Seidel, E. & Okrusch, M., 1977. Chloritoid-bearing metapelites associated with glaucophane rocks in western Crete, Greece. *Contributions to Mineralogy and Petrology*, **60**, 321–324.

Seidel, E., 1981. Fe–Mg-verteilung zurischen koexistierenden karpholithe und chloritoiden. *Fortschritte der Mineralogie*, **59**, 180–181.

Seifert, F., 1970. Low temperature compatibility relations of cordierite in haplopelites of the system K_2O–MgO–Al_2O_3–SiO_2–H_2O. *Journal of Petrology*, **11**, 73–101.

Seifert, F., 1973. Stability of the assemblage cordierite-corundum in the system MgO–Al_2O_3–SiO_2–H_2O. *Contributions to Mineralogy and Petrology*, **41**, 171–178.

Seifert, F., 1974. Stability of sapphirine: A study of the aluminous part of the system MgO-Al_2O–SiO_2–H_2O. *Journal of Geology*, **82**, 173–204.

Seifert, F., 1976. Stability of the assemblage cordierite + K feldspar + quartz. *Contributions to Mineralogy and Petrology*, **57**, 179–185.

Seifert, F. & Schreyer, W., 1970. Low temperature stability limit of Mg-cordierite in the range 1–7 kilobars water pressure. A redetermination. *Contributions to Mineralogy and Petrology*, **27**, 25–238.

Sharp, Z. D., Essene, E. J., Anovitz, L. M., Metz, G. W., Westrum, E. F. Jr., Hemingway, B. S. & Valley, J. W., 1986. The heat capacity of a natural monticellite and phase equilibria in the system CaO–MgO–SiO_2–CO_2. *Geochimica et Cosmochimica Acta*, **50**, 1475–1484.

Shmulovich, K. J., 1974. Experimental study of phase equilibria in the system CaO–Al_2O_3–SiO_2–CO_2. (In Russian). *Geokhimiya*, 1272–1277.

Skinner, B. J., 1966. Thermal expansion. In: *Handbook of Physical Constants* (ed. Clark, S. P.), *Geological Society of America Memoir*, **97**, 75–96.

Skippen, G. B., 1971. Experimental data for reactions in siliceous marbles. *Journal of Geology*, **79**, 457–481.

Slaughter, J., Kerrick, D. M. & Wall, V. J., 1975. Experimental and thermodynamic study of equilibria in the system CaO–MgO–SiO_2–H_2O–CO_2. *American Journal of Science*, **275**, 143–162.

Smyth, F. H. & Adams, L. H., 1923. The system calcium oxide–carbon dioxide. *Journal of the American Chemical Society*, **45**, 1167–1184.

Staudigel, H. & Schreyer, W., 1977. The upper thermal stability of clinochlore at 10–35 kbar $P(H_2O)$. *Contributions to Mineralogy and Petrology*, **61**, 187–198.

Storre, B. & Nitsch, K-H., 1974. Zur stabilität von Margarit im System CaO–Al_2O_3–SiO_2–H_2O. *Contributions to Mineralogy and Petrology*, **43**, 1–24.

Sueno, S., Cameron, M. & Prewitt, C. T., 1976. Orthoferrosilite: High temperature crystal chemistry. *American Mineralogist*, **61**, 38–53.

Suwa, Y., Tamai, Y. & Naka, S., 1976. Stability of synthetic andradite at atmospheric pressure. *American Mineralogist*, **61**, 26–28.

Taylor, L. A., & Bell, P. M., 1970. Thermal expansion of pyrophyllite. *Carnegie Institute of Washington Yearbook*, **69**, 193–194.

Velde, B., 1965. Phengite micas: synthesis, stability, and natural occurrence. *American Journal of Science*, **263**, 886–913.

Viswanathan, K. & Seidel, E., 1979. Crystal chemistry of Fe–Mg Carpholites. *Contributions to Mineralogy and Petrology*, **70**, 41–47.

Walter, L. S., 1963. Experimental studies on Bowen's decarbonation series: 1: *P–T* univariant equilibria of the "monticellite" and "akermanite" reactions. *American Journal of Science*, **261**, 488–450.

Walter, L. S., 1965. Experimental studies on Bowen's decarbonation series III: *P–T* univariant equilibrium of the reaction: spurrite + monticellite = merwinite + calcite and analysis of assemblages found at Crestmore, California. *American Journal of Science*, **263**, 64–77.

Wechsler, B. A. & Prewitt, C. T., 1984. Crystal structure of ilmenite ($FeTiO_3$) at high temperature and at high pressure. *American Mineralogist*, **69**, 176–185.

Weidner, J. R., 1972. Equilibria in the system Fe–C–O part 1: siderite–magnetite–carbon–vapour equilibrium from 500 to 10,000 bars. *American Journal of Science*, **272**, 735–757.

Wendlandt, R. F. & Eggler, D. H., 1980. The origins of potassic magmas: 1: Melting relations in the systems $KAlSiO_4$–Mg_2SiO_4–SiO_2 and $KAlSiO_4$–MgO–SiO_2–CO_2 to 30 kilobars. *American Journal of Science*, **280**, 385–420.

Westrich, H. R. & Holloway, J. R., 1981. Experimental dehydration of pargasite and calculation of its entropy and Gibbs energy. *American Journal of Science*, **281**, 922–934.

Will, T. M., Powell, R., Holland, T. J. B. & Guiraud, M., 1989. Calculated greenschist facies mineral equilibria in the system CaO–MgO–FeO–Al_2O_3–SiO_2–H_2O–CO_2. *Contributions to Mineralogy and Petrology*, in press.

Yin, H.-A. & Greenwood, H. J., 1983. Displacement of equilibria of OH-tremolite and F-tremolite solid solution. I. Determination of the equilibrium *P–T* curve of OH-tremolite. *EOS* (*Transactions of the American Geophysical Union*), **64**, 347.

Yoder, H. S., 1968. Akermanite and related melilite-bearing assemblages. *Carnegie Institute of Washington Yearbook*, **66**, 471–477.

Zharkov, V. A. & Shmulovich, K. I., 1969. High temperature mineral equilibria in the system CaO–SiO_2–CO_2. *Geochemistry International*, **6**, 853–869.

Ziegenbein, D. & Johannes, W., 1974. Wollastonitbildung aus Quartz und Calcit bei Pf = 2, 4, und 6 kb. *Fortschritte der Mineralogie*, **44**, 77–79.

Received 3 February 1989; revision accepted 14 June 1989.

APPENDIX A

Tables A1 and A2 contain examples of full output from the least squares procedure on selected subsets of the data. These tables are equivalent to those in Holland & Powell (1985, appendix B). The symbols are as in the caption to Table 5, except that 'miss' refers to the misfit in T(K), P (kbars), or $\ln K$ according to the context.